

The Emergence of Patterns in Nature and Chaos Theory

Ryan Greenup & James Guerra

October 23, 2020

Contents

1	Introduction	RYAN	3
1.1	A note on Images in this report		3
2	Fractals		3
2.1	Definition of a Fractal	RYAN	3
2.2	Fractals Generally	JAMES	4
2.3	Fractal Dimension		5
2.3.1	Topological Equivalence	RYAN	5
2.3.2	Hausdorff Measure	RYAN	7
2.3.3	Hausdorff Dimension	RYAN	10
2.3.4	Box Counting Dimension	JAMES	11
2.4	Generating Self Similar Fractals	RYAN	13
2.4.1	Vicsek Fractal		13
2.4.2	Turtle		19
2.4.3	Pascals Triangle and Sierpinski's Triangle	JAMES	19
2.5	Fractal Dimensions Sans Self Similarity	RYAN	25
3	Connecting Fractals to Natural Processes	RYAN	26
3.1	Constructing a Simple Process		26
3.2	The Fibonacci Numbers		26
3.3	The Dimension of the Fractal		29
4	The Fibonacci Sequence and the Golden Ratio		29
4.1	The Golden Ratio	RYAN	29
4.2	Golden Ratio In terms of the Fibonacci Sequence		30
4.2.1	Prove that the Sequence is Bounded	JAMES	31
4.2.2	Find the Limit	JAMES	33
4.3	Comments	RYAN	34
4.3.1	Equivalent forms of the Golden Ratio		34
4.4	A closed Solution for the Fibonacci Numbers	RYAN	35
4.4.1	Golden Ratio		37
4.5	Sunflower Seeds; Fibonacci Numbers in Nature	RYAN	37

CONTENTS

5 Julia Sets	RYAN 38
5.1 Introduction	38
5.2 Motivation	40
5.3 Plotting the Sets	40
5.4 Dimension of the Julia Set	43
6 Mandelbrot Set	RYAN 51
7 Conclusion	RYAN 53
A Appendix	55
A.1 Code Listings	55
A.2 Resources Used for the Hausdorff Dimension	56
A.3 Functions for constructing the Julia Set	57
A.4 Exponential Generating Functions	60

1 Introduction

RYAN

Fractals are complex shapes that often occur from natural processes, in this report we hope to investigate the emergence of patterns and complex structures from natural phenomena. We begin with an investigation into fractals and the concept of dimension and then discuss links between fractal patterns and natural processes.

1.1 A note on Images in this report

Although the images in this document may appear to be quite small, they are high quality PNG images and one of the luxuries of PDF is that the embedded media is near lossless, so to perceive greater detail in an image it is sufficient to simply zoom in and the greater detail should be rendered.¹

2 Fractals

2.1 Definition of a Fractal

RYAN

Benoît Mandelbrot coined the term fractal in 1975 [20] and defined it his 1982 book *The Fractal Geometry of Nature* [37, p. 15] :

A fractal is by definition a set for which the Hausdorff Besicovitch dimension strictly exceeds the topological dimension.

*Every set with a non-integer D is a fractal.*²

The topological dimension is a strictly integer value that describes the natural dimension used to describe a shape [53], for example the *Koch Snowflake* (shown in Figure 2) is composed of just a line, so its topological dimension would simply be 1, its *fractal dimension* however is shown to be $\frac{\ln(4)}{\ln(3)}$ at (8) in §2.3.1.

Many authors seem to accept this earlier definition (see e.g. [59, §2.2] and [57, §2.1]), this definition however does not capture many edge-case fractals [12, p. VII] and in reprinting of *The Fractal Geometry of Nature* Mandelbrot himself commented that in hindsight it may have been more appropriate [37, p. 459]:

to leave the term “fractal” without a pedantic definition, to use “fractal dimension” as a generic term applicable to all the variants in Chapter 39, and to use in each specific case whichever definition is the most appropriate.

¹Apparently it's also possible to embed live GIFs into PDF as well which would have been nice to do had time permitted, see for example the *Animate* package for L^AT_EX[11] and [this discussion](#) [46] generally.

²In this quote by Mandelbrot is indicating that by the earlier definition of a fractal, any shape (i.e. a subset of \mathbb{R}^n) with a non-integer dimension must be a fractal. This however is merely a sufficient, rather than a necessary, condition of a fractal, for example the *Dragon Curve* discussed in section 2.4.2 and the Mandlebrot set discussed at section 6 both have a dimension of 2 but are clearly fractals by this definition because their shape is constructed with a line, which has a “topological” dimension of 1.

Gerald Edgar, in his 2008 book *Measure, topology, and fractal geometry* rejected this view because “*a term without a ‘pedantic definition’ cannot be studied mathematically*” [12, p. VII] and presented a more robust definition in Ch. 6 of that book, it was however accepted that the loose definition of fractal dimension is convenient and was indeed adopted in that work.

Although reviewing the precise definition of a fractal would have been very interesting, without a cursory knowledge of fractals generally this would have been very time consuming and outside the scope of this report³.

Some authors simply define a fractal as a shape that *shows irregularities at all scales* [21, p. 1] and in his 2003 book, *Fractal Geometry*, Facloner suggested that it is more convenient to describe a fractal by a list of properties characteristic of such shapes⁴ because of the difficulty in defining a fractal in a way that can encompass all edge cases and provides the following characteristics [14, p. xxv]:

- Detail at all scales
- Cannot be described in a traditional geometric way
- May have some form of approximate self similarity
- Usually the fractal dimension is greater than its topological dimension
- In many cases defined very simply, perhaps recursively

This will be the approach adopted in this report.

It's interesting to note that many authors refer to complex natural shapes as fractals, such as coastlines (see e.g. [24, 63, 62]) much in the spirit of Mandelbrot's paper *How long is the Coastline of Britain* [36], although he coined the term fractal many years after this paper, presumably he might have had this in mind⁵ when framing the definition so this issue in clearly defining what a fractal is appears on the surface to be a purely mathematical one (as opposed to a practical or applied one).

The Wikipedia page on fractals [17] also points out that a fractal is nowhere differentiable, this would be because a fractal is nowhere smooth, which is certainly an important and distinguishing feature worth noting.

2.2 Fractals Generally

JAMES

Dimension is the main defining property of a fractal. As aforementioned above, the Hausdorff dimension is a unique number in that, if we take some shape in \mathbb{R}^n , and the Hausdorff dimension converges to some number, then the dimension of the shape is given by that number. Otherwise, it will equal 0 or ∞ . For example, if we want to evaluate the dimension of a square and we use a 1-Dimensional shape as the cover set

³Mandelbrot also discussed fractals of a Euclidean and Reimannian nature, [37, p. 361], this again is interesting but too specific for the broad nature of our investigation

⁴Much like the definition of life in the field of biology

⁵Mandelbrot also spent much time looking at the roughness of financial markets and so presumably may have had that in mind as well, see e.g. [20, 38]

to calculate the Hausdorff dimension, we will get ∞ . On the other hand, if we do the same with a 3-Dimensional shape, we will get 0. And finally if we use a 2-Dimensional shape, the Hausdorff dimension will evaluate to 2. This same notion is important when computing the dimension of a more complex shape such as the Koch snowflake.

To define a fractal, we must define it's dimension. Whilst some research states that a fractal has a non-integer dimension, this is not true for all fractals. Although, most fractals like the Koch snowflake do in fact have non-integer dimensions, we can easily find a counter example namely, the Mandelbrot set. The Mandelbrot set lies in the same dimension as a square, a 2-Dimensional shape. However, we give recognition to the complexity and roughness of the Mandelbrot set which clearly distinguishes itself from a square. Beneath the Mandelbrot set's complexity are exact replicates of the largest scaled Mandelbrot set, i.e a self similar shape. Furthermore, although the Mandelbrot set has an integer dimension, the self similarity and complexity is what also defines its fractal nature.

2.3 Fractal Dimension

The concept of a non-integer dimension may at first seem odd, particularly given that the familiar definition from linear algebra (concerned with the number of vectors within a basis for a vector space [30]) is strictly an integer value, but in the early 20th century mathematicians recognized the shortcomings of this definition [37, Ch. 3].

In this section we hope to convince the reader that there is grounds for extending the definition of dimension and as a matter of fact many definitions for non-integer dimensions of a shape have been proposed (see generally [37, Ch. 39] and [21, §1.3]) of these the Hausdorff Dimension (and corresponding Hausdorff Measure) is considered to be the most important and mathematically robust [14, p. 27], while the *Box-Counting Dimension* (introduced in §2.3.4) has the most practical applications in science [47, p. 192].

The Hausdorff dimension is more like counting balls than boxes and is identical to the Box-Counting Dimension in many cases, it's more general but harder to define [53]. An extension to the work of this report would be to show the mathematical connections between the Hausdorff Dimension and box counting dimension with respect to the fractals generated and measured.

2.3.1 Topological Equivalence

RYAN

Topology is an area of mathematics concerned with ideas of continuity through the study of figures that are preserved under homeomorphic transformations [18] , where two figures are said to be homeomorphic if there is a continuous bijective mapping between the two shapes [47, p. 105] . ⁶

So for example deforming a cube into a sphere would be homeomorphic, but deforming a sphere into a torus would not, because the the surface of the shape would have to be compromised to achieve that.

⁶For further reading on this topic see [47, p. 106]

As mentioned above, historically, the concept of dimension was a difficult problem with a tenuous definition. Although an intuitive definition related the dimension of a shape to the number of parameters needed to describe that shape, this definition is not sufficient to be preserved under a homeomorphic transform.

Consider the Koch fractal and snowflake in Figures 1 and 2, at each iteration (n) the perimeter is given by $p_n = \left(\frac{4}{3}\right) p_{n-1}$ and the number of edges by N_n :

$$N_n = N_{n-1} \cdot 4 \quad (1)$$

$$= 3 \cdot 4^n \quad (2)$$

If the length of any individual side was given by l and scaled by some value s then the length of each individual edge would be given by:

$$l = \frac{s \cdot l_0}{3^n} \quad (3)$$

The total perimeter would be given by:

$$p_n = N_n \times l \quad (4)$$

$$= 3 \cdot 4^n \times \frac{s \cdot l_0}{3^n} \quad (5)$$

$$= 3 \cdot s \cdot l_0 \left(\frac{4}{3}\right)^n \quad (6)$$

$$\implies p_n \cdot s \propto \left(\frac{4}{3}\right)^n \quad (7)$$

$$\implies n = \frac{\log(4)}{\log(3)} \approx 1.26 \quad (8)$$

This means that if the Koch Snowflake is scaled by any factor, the resulting perimeter of the snowflake will not be linearly proportional to the scaling factor, as would be the case with an ordinary shape such as a square or a circle, it will instead be proportional to 1.26, this should hopefully motivate the need to more clearly define both the concept of measure (in this case the perimeter⁷) and dimension.

To clarify the Koch snowflake, is defined such that there are no edges, every point on the “curve” is the vertex of an equilateral triangle, this shape has no smooth edges.

See [55, p. 414] and [2, §5.4] for further reading on the self similar dimension of the *Koch Snowflake*.

This approach of considering the scaling factor of a deterministic fractal is known as the similarity dimension [55, p. 413] and should be equal to the Hausdorff and box counting dimensions for most fractals. For fractals that aren’t so obviously self similar

⁷Grant Sanderson equates the measure of a fractal as analogous to mass, which is a very helpful way comparison [53]

2.3 Fractal Dimension

it won't be feasible however [33, p. 393], for example with the Julia Set ⁸ or the outline of a coastline it is not immediately clear if the the dimension would be constant at all scales

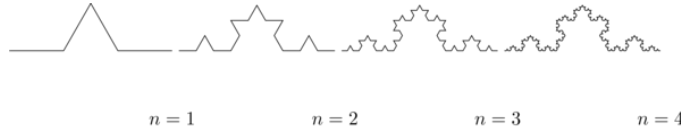


Figure 1: Progression of the Koch Snowflake

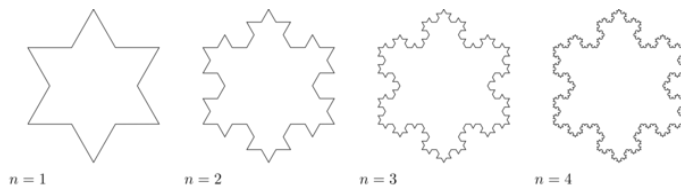


Figure 2: Progression of the Koch Snowflake

2.3.2 Hausdorff Measure

RYAN

The Hausdorff dimension depends first on a rigorous definition of measure, this is distinct from the box counting approach in that it is more mathematically rigorous, it is however complex and in practice this report will be concerned with implementing the box counting dimension. ⁹

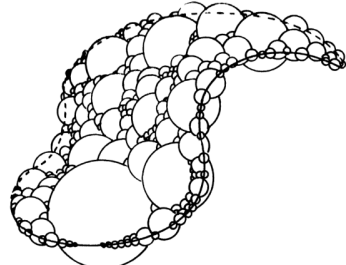


Figure 3: The Hausdorff Measure of an arbitrary surface approximated by the cross section of balls with diameter $< \delta$, this is reproduced from *Measure, Topology and Fractal Geometry* [12, p. 166].

Let F be some arbitrary subset of euclidean space \mathbb{R}^n , ¹⁰

Let U be a subset of euclidean space \mathbb{R}^n such that the diameter is defined as the greatest distance between any of the points:

$$|U| = \sup (\{|x - y| : x, y \in U\})$$

Consider a collection of these sets, $G = \{U_i : i \in \mathbb{Z}^+\}$ such that each element has a diameter less than δ .

The motivating idea is that if the elements of G can be laid on-top of F then

⁸It is indeed shown to be mostly constant at all scales in section §

⁹See §A.2 for further reading.

¹⁰A subset of euclidean space could be interpreted as an uncountable set containing all points describing that region

G is said to be a δ -cover of F , more rigorously, G is a δ -cover of F if:¹¹

$$F \subset \bigcup_{U \in G} (U) \quad : \quad 0 \leq |U| \leq \delta \quad (9)$$

An example of this covering is provided in Figure 4, in that example the figure on the right is covered by squares, which each could be an element of $\{U_i\}$, it is important to note, by this definition, that the shapes represented by U could be any arbitrary figure [14, §2.1] the size of which may vary in size so long as the diameter is less than δ .

So for example:

- F could be some arbitrary 2D shape, and U_i could be a collection of identical squares, OR
- F could be the outline of a coastline and U_i could be a set of circles, OR
- F could be the surface of a sheet and U_i could be a set of spherical balls as shown in Figure 3
 - Some authors suggest that the Hausdorff Measure is concerned primarily with round covering objects (see e.g. [53]), this is well illustrated by Figure 3, however in truth it is merely more convenient to use round shapes for most fractals.
 - The use of balls is a simpler but equivalent approach to the theory [14, §2.4] because any set of diameter r can be enclosed in a ball of radius $\frac{r}{2}$ [13, p. 166]
- F could be a more abstracted figure like Figures 4 or 6 and $\{U_i\}$ a collection of various different lines, shapes or 3d objects.

The Hausdorff measure is concerned with only the diameter of each element of $\{U_i\}$ and considers $\sum_{U \in G} [|U|^s]$ where each element $U \in G$ is arranged so as to minimize the value of the summation [14, p. 27], the δ -Hausdorff is hence defined, for various dimensions s :

$$\mathcal{H}_\delta^s(F) = \inf \left\{ \sum_{U \in G} |U|^s : \{U_i\} \text{ is a } \delta\text{-cover of } F \right\}, \quad \delta, s > 0 \quad (10)$$

¹¹Falconer defines this as $\bigcup_{i=1}^{\infty} [14, §2.1]$, presumably treating any index value greater than the cardinality of the set as \emptyset , this is particularly ambiguous and we have avoided it, an alternative way to present that might be $\bigcup_{i=0}^{\#G}$ where $\#G$ denotes the cardinality of G (or ∞ if it is uncountable). The use of $\#\square$ to denote cardinality was introduced by Knuth in *Concrete Mathematics* [22] and is convenient in that it avoids any ambiguity with diameter ($|\square|$).

The value of s can be different regardless of the dimension of F , for example if F was an arbitrary 2D shape the value of $\mathcal{H}_\delta^2(F)$ is equivalent to considering the number of shapes $U \in G$ (e.g. boxes, discs etc.), of diameter $\leq \delta$ that will cover over a shape as shown in Figure 4, the delta Hausdorff measure $\mathcal{H}_\delta^2(F)$ will be the area of the boxes when arranged in such a way that minimizes the area.

As δ is made arbitrarily small \mathcal{H}_δ^s will approach some limit, in the case of Figures 4 and 6 the value of \mathcal{H}_δ^2 will approach the area of the shape as $\delta \rightarrow 0$ and so the s^{th} dimensional Hausdorff measure is given by:

$$\mathcal{H}^s = \lim_{\delta \rightarrow 0} (\mathcal{H}_\delta^s) \quad (11)$$

This is defined for all subsets of \mathbb{R}^n for example the value of \mathcal{H}^2 corresponding to Figure 6 will be limit that boxes would approach when covering that area, which would be the area of the shape ($4 \times 1^2 + 4 \times \pi \times \frac{1}{2^2} + \frac{1}{2} \times 1 \times \sin \frac{\pi}{3}$).

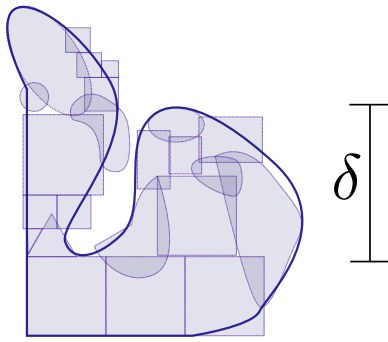


Figure 4: The blue outline corresponds to some $F \subset \mathbb{R}^2$, covered by various grey objects, each of which represent an element from the set U_i . The grey shapes all have a diameter less than δ and so this $\bigcup [U_i]$ would be a δ -covering of F .

Lower Dimension Hausdorff Measurements

Examples Consider again the example of a 2D shape, the value of \mathcal{H}^1 would still be defined by (10), but unlike \mathcal{H}^2 in §2.3.2 the value of $|U_i|^1$ would be considered as opposed to $|U_i|^2$ (i.e. the diameter as opposed to the diameter squared).

As δ is made arbitrarily small the boxes¹² that cover the shape are made also to be arbitrarily small. Although the area of the boxes must clearly be bounded by the shape of F , if one imagines an infinite number of infinitely dense lines packing into a 2D shape with an infinite density it can be seen that the total length of those lines will be infinite

and so the limit in (11) will increase without bound.

To build on that same analogy, another way to imagine this is to pack a 2D shape with straight lines, the total length of all lines will approach the same value as the length of the lines of the squares as they are packed infinitely densely. Because lines cannot fill a 2D shape, as the density of the lines increases, the overall length will increase without bound.

¹²Even though U may contain a variety of shapes, (10) is concerned only with the power of their diameter, so in this sense the limit is concerned only with boxes corresponding to the diameter of the elements of U

This is consistent with fractals as well, consider the Koch snowflake introduced in section 2.3.1 and shown in Figure 1, the dimension of this shape, as shown in §2.3.1 is greater than 1, and the number of lines necessary to describe that shape is also infinite because every point of the “curve” is a point of an equilateral triangle.

Formally If the dimension of F is less than s , the Hausdorff Measure will be given by:

$$\dim(F) < s \implies \mathcal{H}^s(F) = \infty \quad (12)$$

Higher Dimension Hausdorff Dimension For small values of s (i.e. less than the dimension of F), the value of \mathcal{H}^s will be ∞ .

Consider some value s such that the Hausdorff measure is not infinite, i.e. values of s :

$$\mathcal{H}^s = L \in \mathbb{R}$$

Consider a dimensional value t that is larger than s and observe that:

$$\begin{aligned} 0 < s < t &\implies \sum_i [|U_i|^t] = \sum_i [|U_i|^{t-s} \cdot |U_i|^s] \\ &\leq \sum_i [\delta^{t-s} \cdot |U_i|^s] \\ &= \delta^{t-s} \sum_i [|U_i|^s] \end{aligned}$$

Now if $\lim_{\delta \rightarrow 0} [\sum_i |U_i|^s]$ is defined as a non-infinite value:

$$\lim_{\delta \rightarrow 0} \left(\sum_i [|U_i|^t] \right) \leq \lim_{\delta} \left(\delta^{t-s} \sum_i [|U_i|^s] \right) \quad (13)$$

$$\leq \lim_{\delta \rightarrow 0} (\delta^{t-s}) \cdot \lim_{\delta \rightarrow 0} \left(\sum_i [|U_i|^s] \right) \quad (14)$$

$$\leq 0 \quad (15)$$

and so we have the following relationship:

$$\mathcal{H}^s(F) \in \mathbb{R}^+ \implies \mathcal{H}^t(F) = 0 \quad \forall t > s \quad (16)$$

Hence the value of the s -dimensional *Hausdorff Measure*, s is only a finite, non-zero value, when $s = \dim_H(F)$.

2.3.3 Hausdorff Dimension

RYAN

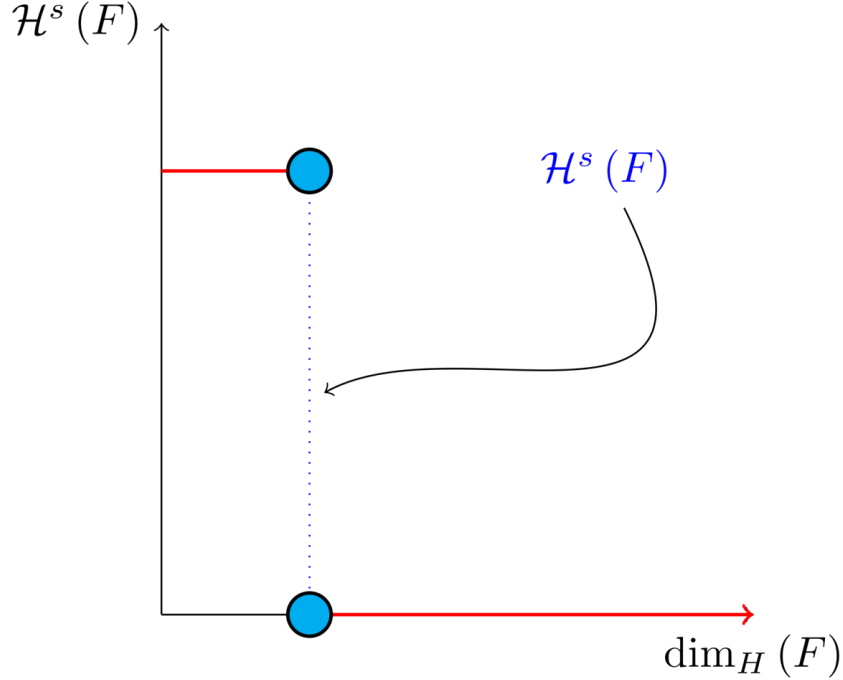


Figure 5: The value of the s -dimensional *Hausdorff Measure* of some subset of *Euclidean space* $F \in \mathbb{R}^n$ is 0 or ∞ when the dimension of F is not equal to s .

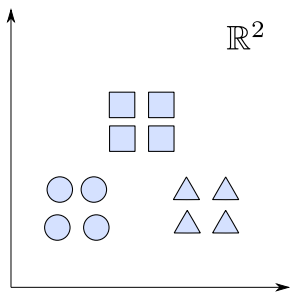


Figure 6: A disconnected subset of \mathbb{R}^2 , the squares have a diameter of $\sqrt{2}$, the circles 1 and the equilateral triangles 1.

The value s at which $\mathcal{H}^s(F)$ changes from ∞ to 0, shown in Figure 5, is the defined to be the *Hausdorff Dimension* [14, §2.2], it is a generalization of the idea of dimension that is typically understood with respect to ordinary figures.

2.3.4 Box Counting Dimension JAMES

While the Hausdorff dimension is the first formal definition to measure the roughness of a fractal, there are several other definitions of dimension that have stemmed from this. Namely, the box-counting dimension. The box counting

method is widely used as it is relatively easy to calculate [14, p. 41] and in many cases is equal to the *Hausdorff Dimension* [39, p. 11] (see generally [34]). The box-counting dimension is defined as the following from [15]:

Let F be any non-empty bounded subset of \mathbb{R}^n and let $N_\delta(F)$ be the smallest number of sets of diameter at most δ which can cover F . The *lower* and *upper* box-counting dimensions of F respectively are defined as

$$\underline{\dim}_B F = \lim_{\delta \rightarrow 0} \frac{\ln N_\delta(F)}{-\ln \delta}$$

$$\overline{\dim}_B F = \lim_{\delta \rightarrow 0} \frac{\ln N_\delta(F)}{-\ln \delta}$$

When the *lower* and *upper* box-counting dimensions of F are equal, then

$$\dim_B F = \lim_{\delta \rightarrow 0} \frac{\ln N_\delta(F)}{-\ln \delta}$$

For example, suppose we had a square with side length 1 and we use smaller squares of side length $\frac{1}{\delta}$ to cover the larger square. This would mean that one side of the large square would need $\delta \frac{1}{\delta}$ small squares, and so to cover the entire square, one would need n^2 small squares, i.e. $N_{\frac{1}{n}}(F) = n^2$. Now, substituting these values into the box-counting definition, we get:

$$\begin{aligned} \dim_B F &= \lim_{\frac{1}{\delta} \rightarrow 0} \frac{\ln(\delta^2)}{-\ln(\frac{1}{\delta})} \\ &= \lim_{\frac{1}{\delta} \rightarrow 0} \frac{\ln(\delta^2)}{\ln(\delta)} \\ &= \lim_{\frac{1}{\delta} \rightarrow 0} 2 \frac{\ln(\delta)}{\ln(\delta)} \\ &= 2 \end{aligned}$$

Which is expected, because we know that a square is a 2-Dimensional shape. We can apply this same concept to fractals. Consider another example, the Koch Curve, a self similar fractal which we can calculate its dimension and provide a measure of roughness of the curve. If we take a close look at the curve progression in Figure 1, the pattern begins with one line segment and the middle third of the line is replaced with two sides of an equilateral triangle with side length $\frac{1}{3}$. After this first iteration, the line segment now becomes four line segments. Thus, if we use a square of length $\frac{1}{3^\delta}$ to cover the δ^{th} iteration of the curve, there will be 4^δ line segments covered.

Let F be the Koch Curve.

$$\begin{aligned} \dim_B F &= \lim_{\frac{1}{3^\delta} \rightarrow 0} \frac{\ln(4^\delta)}{-\ln(\frac{1}{3^\delta})} \\ &= \lim_{\frac{1}{3^\delta} \rightarrow 0} \frac{\ln(4^\delta)}{\ln(3^\delta)} \\ &= \lim_{\frac{1}{3^\delta} \rightarrow 0} \frac{\ln(4)}{\ln(3)} \\ &= \frac{\ln(4)}{\ln(3)} \end{aligned}$$

2.4 Generating Self Similar Fractals

RYAN

In order to investigate the dimension of fractals, we intend to generate and measure a variety of figures by using of *R* [50], *Julia* [4] and *Python* [61].

Self Similar fractals have a self-similar dimension and so can be used to verify an approach implemented with a programming language.

2.4.1 Vicsek Fractal

The Vicsek Fractal [59, p. 12] involves a pattern of iterating boxes, to implement this consider the process¹³:

$$\mathbf{B} \leftarrow \begin{bmatrix} \mathbf{B} & \mathbf{Z} & \mathbf{B} \\ \mathbf{Z} & \mathbf{B} & \mathbf{Z} \\ \mathbf{B} & \mathbf{Z} & \mathbf{B} \end{bmatrix} \quad (17)$$

where:

- $\mathbf{B} = [1]$
- $\mathbf{Z} = [0]$

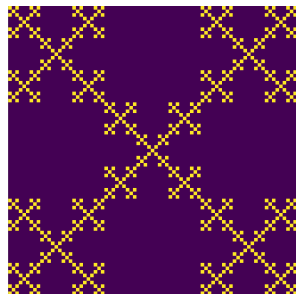


Figure 7: Vicsek fractal [59, p. 12] (also known as the *Anti-Cross-Stitch* [23]) produced by listing 1, at each iterative step the fractal itself is “copied” to the four corners of itself producing this complex shape.

If this is repeated many times a matrix of values will be created, such a matrix can be interpreted as a greyscale image and plotted as a heat-map to show the fractal (shown in Figure).

The iterative process shown in (17) is represented as a recursive function at line 5 of listing 1 and visualized at line 22. To measure the the dimension of this fractal a the sum of the matrix is taken to be the measure of the fractal, two fractals are generated and the change in size relative to the scale is compared and the log taken to return the value of the dimension:

$$\mathcal{D} = \frac{s}{m_2/m_1}$$

The recursive function begins with a 3x3 matrix, where the four corner squares and middle square are set to 1 and the rest are set to 0, a new matrix is built by joining

¹³This was actually a fractal I came up with myself only to later find that somebody already had the same idea!

together the past matrix following the rule described in (17). The function repeats until it reaches some arbitrary set width.

At each step of the process, the number of elements of this fractal increases by a ratio of 5 while the height increases only by a factor of 3, hence the self similarity dimension is given by:

$$\begin{aligned} 5 &= 3^D \\ \implies D &= \frac{\ln 5}{\ln 3} \end{aligned} \quad (18)$$

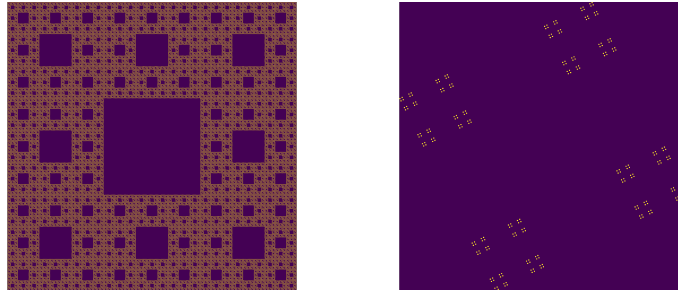
By modifying listing 1 alternative fractals can get also be generated like *Cantor's Dust* and *Sierpinski's Carpet* shown in Figures and .

Upon review this is actually a variant on the *Cantor Dust* which should actually be represented by a 3×3 matrix:

$$\mathbf{B} \leftarrow \begin{bmatrix} \mathbf{B} & \mathbf{Z} & \mathbf{B} \\ \mathbf{Z} & \mathbf{Z} & \mathbf{Z} \\ \mathbf{B} & \mathbf{Z} & \mathbf{B} \end{bmatrix} \quad (19)$$

and hence has the same dimension as the *Vicsek Fractal* as opposed to a dimension of 1.

Sierpinskis Carpet and Cantor's Dust By modifying the approach provided in listing 1 other fractals such as *Sierpinski's Carpet* and *Cantor's Dust* can be produced, this is implemented in listings 18 19 and shown in Figures 2.4.1 and respectively. ¹⁴



Sierpinski's Triangle Not all fractal patterns can be produced by using recursive functions involving matrices, one such function is *Sierpinski's Triangle*.

Chaos Game The chaos game is a technique that can generate fractals, one of the advantages of this approach is that it can provide an estimate of the theoretical measure of a fractal without needing to iterate a function many times. The technique involves marking 3 points of an equilateral triangle and marking an arbitrary point,

¹⁴See generally Ch. 2.7 of [47, §2.7] for further Reading and [37, p. 79] for further reading on Cantor.

```

1  #-----
2  #--- Function ---
3  #
4  function vicsek_matrix(ICMat, width)
5      B = ICMat
6      h  = size(B)[1]
7      w  = size(B)[2]
8      Z  = zeros(Int, h, w)
9      B = [B Z B ;
10         Z B Z ;
11         B Z B]
12      if (3*w)<width
13          B = vicsek_matrix(B, width)
14      end
15      return B
16  end
17  #
18  #--- Plot ---
19  #
20  #
21  (mat = vicsek_matrix(fill(1, 1, 1), 27)) |> size
22  GR.imshow(mat)
23  #
24  #-----
25  #--- Similarity Dimension ---
26  #
27  #
28  mat2 = vicsek_matrix(fill(1, 1, 1), 1000)
29  l2   = sum(mat2)
30  size2 = size(mat2)[1]
31  #
32  mat1 = vicsek_matrix(fill(1, 1, 1), 500)
33  l1   = sum(mat1)
34  size1 = size(mat1)[1]
35  #
36  #
37  julia> log(l2/l1)/log(size2/size1)
38  1.4649735207179269
39  julia> log(5)/log(3)
40  1.4649735207179269

```

Listing 1: Generating the Vicsek Fractal (shown in Figure 7) and measuring the dimension using *Julia*, the measured dimension is consistent with the self similarity dimension shown in (18)

select one of these 3 points randomly with a uniform probability and create a new point halfway between the previous point and this point, repeat this process for as many points of detail are desired for the image.

This can be visualized by mapping the co-ordinates of an equilateral triangle to a Cartesian plane:

- $A (0, 0)$
- $B (0, 1)$
- $C (0.5, \sin(\frac{\pi}{3}))$

The mean value of the x, y values for these co-ordinates is equal to the halfway point and using this the chaos game can be implemented as a program and visualized by plotting each point on a scatter plot. This is implemented in **R** in listing 2 and the output is shown in Figure 8.

To measure the fractal dimension of this could be done by mapping the Cartesian plane back to a matrix and taking the same approach as previous fractals presented, this however was not implemented, due to time constraints, the dimension was however measured using the method discussed at §2.4.1.

```
1 library(ggplot2)
2 # Parameters
3 n <- 50000
4 df <- data.frame("xval"=1:n, "yval"=1:n)
5 # Constants
6 x <- c(runif(1), runif(1))
7 A <- c(0, 0)
8 B <- c(1, 0)
9 C <- c(0.5, sin(pi/3))
10 # Loop
11 for (i in 1:n) {
12   dice = sample(1:3, 1)
13   if (dice == 1) {
14     x <- (x + A)/2
15     df[i,] <- x
16   } else if (dice == 2) {
17     x <- (x + B)/2
18     df[i,] <- x
19   } else {
20     x <- (x + C)/2
21     df[i,] <- x
22   }
23 }
24 # Plot
25 ggplot(df, aes(x = xval, y = yval)) +
26   geom_point(size = 1, col = "cadet blue") +
27   theme_classic()
```

Listing 2: R code to construct Sierpinski's triangle through the Chaos Game, shown in Figure 8.

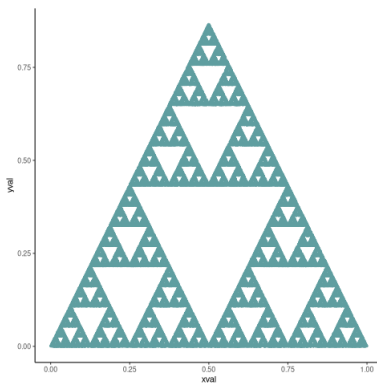


Figure 8: Sierpinski's Triangle created using the *Chaos Game* in listing 2.

an equilateral *Sierpinski's Triangle*, it does however converge to this value slowly.

Pascals Triangle

RYAN

The even and odd values in *Pascal's Triangle* demonstrate the same pattern as the *Sierpinski Triangle* this is discussed in greater detail in §2.4.3, implementing this to produce the sierpinski triangle is very simple, it is however significantly more resource intensive, even in *Julia* than using the chaos game and the measured dimension converges to the self similar dimension very slowly.

The fractal produced is composed of right angle triangles, as opposed to equilateral triangles but interestingly the measured dimension is still the same as

```

1  function pascal(n)
2      mat = [isodd(binomial(BigInt(j+i),BigInt(i))) for i in 0:n, j in 0:n]
3      return mat
4  end
5  GR.imshow(pascal(999))
6  GR.savefig("../Report/media/pascal-sierpinsky-triangle.png")
7
8  #-----
9  #-- Calculate Dimension --
10 #-----
11
12 mat2 = pascal(300)
13 l2 = sum(mat2)
14 size2 = size(mat2)[1]
15 mat1 = pascal(200)
16 l1 = sum(mat1)
17 size1 = size(mat1)[1]
18 log(l2/l1)/log(size2/size1)
19 # https://en.wikipedia.org/wiki/Sierpi%C5%84ski\_triangle
20 log(3)/log(2)
21
22 #-----
23 julia> log(l2/l1)/log(size2/size1)
24 1.8177195595512954
25 julia> log(3)/log(2)
26 1.5849625007211563

```

Listing 3: Julia code demonstrating Sierpinski's triangle, this converges to the self similar dimension very slowly, using the ratio between a 3000^2 and 2000^2 matrix gave the correct answer to 2 decimal places, using a 300^2 and 200^2 matrix produced a value far off as shown.

2.4.2 Turtle

Some Fractals cannot be well explained by using matrices or the chaos game, Turtle graphics are a programmatic way to draw a pen across a screen, these are implemented in *Julia* using the *Luxor* package [27].

We were unfortunately unable to implement a strategy to measure the dimension of such fractals, one such approach that looked promising but did not return consistent results was to export the generated image to a PNG and then import that file as a matrix using the *Python Pillow Library* [48] or the *Julia Images* library [28], when this was unsuccessful we also experimented with *ImageMagick* [35], *AstroPy* [1] and *JuliaAstro* [26]. Unfortunately the values returned by this approach were inconsistent and further investigation into this method is required.

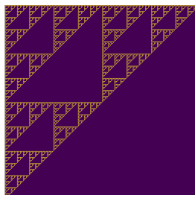


Figure 10: Sierpinski's triangle generated

and shown in Figure .

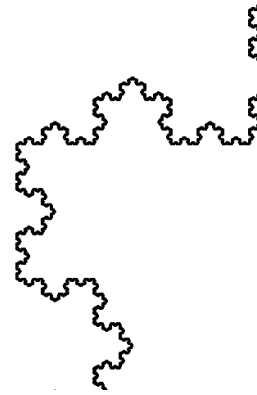


Figure 9: Portion of the Koch Snowflake Produced by the Turtle graphics in listing 4

The koch snowflake can be implemented by recursively calling a function that draws the first level of a koch curve, if this function decrements a provided level and is defined to call itself for each arm of the curve unless the level has reached zero it will produce a koch snowflake at the specified level, this is implemented in listing 4 and shown in Figure 9.

The dragon curve is slightly more complicated and can be implemented by two separate functions, one to turn and trigger a motion and the other to control in which direction to turn, this is implemented in *Julia* in listing 5

2.4.3 Pascals Triangle and Sierpinski's Triangle

Motivation Over many centuries, mathematicians have been able to produce a range of patterns from Pascal's triangle. One of which is relevant to the emergence of Sierpinski's triangle. To construct Pascal's triangle it begins with a 1 in the 0th (top) row, then each row underneath is made up of the sum of the numbers directly above it, see Figure ???. Alternatively, the n^{th} row and k^{th} column can be written in combinatorics form, $\binom{n}{k} = \binom{n-1}{k-1} + \binom{n-1}{k}$.

```
1  using Shapefile
2  using Luxor
3  using Pkg
4
5  #-----
6  #--- Round Snowflake Working ---
7  #-----
8  function snowflake(length, level, a)
9      if level == 0
10         Forward(a, length)
11         Circle(a, 1)
12         return
13     end
14     length = length/9
15     snowflake(length, level-1, a)
16     Turn(a, -60)
17     snowflake(length, level-1, a)
18     Turn(a, 2*60)
19     snowflake(length, level-1, a)
20     Turn(a, -60)
21     snowflake(length, level-1, a)
22 end
23
24 a = Turtle()
25 @png begin
26 for i in 1:3
27     levels = 9
28
29     Pendown(a)
30     snowflake(8^(levels-1), levels, a)
31     Turn(a, 120)
32 end
33 end 600 600 "snowCurve.png"
```

Listing 4: Generate a Koch Snowflake using a Turtle Diagram

```

1  using Shapefile
2  using Luxor
3
4  #-----
5  #--- Dragon -----
6  #-----
7  # Define the Parent Function
8  function dragon(®, order, length)
9      print(" ") # Don't remove this or code breaks, I don't know why?
10     Turn(®, order*45)
11     dragon_iterate(®, order, length, 1)
12 end
13 # Define the Helper Function
14 function dragon_iterate(®, order, length, sign)
15     if order==0
16         Forward(®, length)
17     else
18         rootHalf = sqrt(0.5)
19         dragon_iterate(®, order -1, length*rootHalf, 1)
20         Turn(®, sign * -90)

21         dragon_iterate(®, order -1, length*rootHalf, -1)
22     end
23 end
24 # Draw the Image
25 @png begin
26     ® = Turtle()
27     # Start from left to centre result
28     Turn(®, 180)
29     Penup(®)
30     Forward(®, 200)
31     Pendown(®)
32     Turn(®, 180)
33     # Create the Output
34     dragon(®, 15, 400)
35 end 1000 1000
36
37 # Create many images
38 ;mkdir /tmp/dragon
39 for i in range(1, 15)
40     name = string("/tmp/dragon/d", lpad(d, 5, "0"), ".png")

41 @png begin
42     ® = Turtle()
43     # Start from left to centre result
44     Turn(®, 180)
45     Penup(®)
46     Forward(®, 200)
47     Pendown(®)
48     Turn(®, 180)
49     # Create the Output
50     dragon(®, 15, 400)
51 end 1000 1000 name
52 end
53 montage -geometry 1000x1000 *.png dragon.png

```

Listing 5: Julia code to produce the Dragon Curve shown in Figure 11

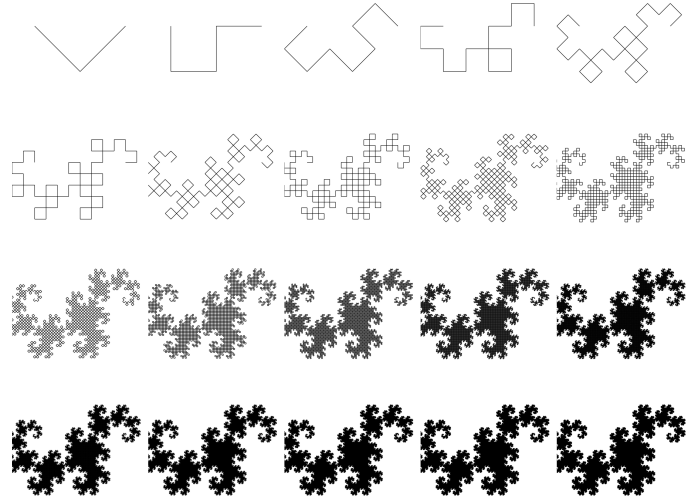
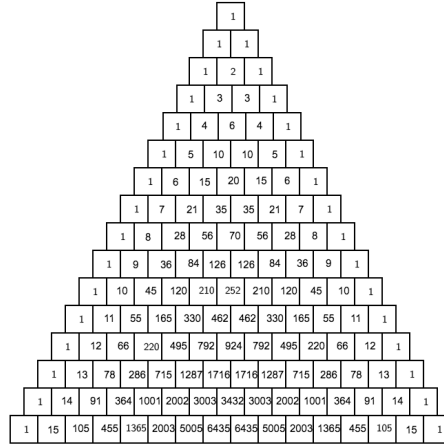


Figure 11: Progression of the Dragon Curve, this is known as a space filling curve [47, p. 350] which is a curve with a range that contains the entire 2-dimensional unit square [58], it has a dimension of two. For some historical background on the curve on the origins of this curve see [56].



The connection As mentioned before there is one pattern that produces the Sierpinski triangle, namely highlighting all odd numbers in Pascal's triangle. This is equivalent to considering all the numbers in the triangle modulo 2, shown in Figure 12.

In Figure 12, we can observe that all the highlighted odd numbers begin to form the Sierpinski triangle. Note that this is not the complete Sierpinski's triangle, that would require an infinite number of iterations. Now, we also notice that there are three identical Sierpinski triangles within the larger triangle, each containing the same

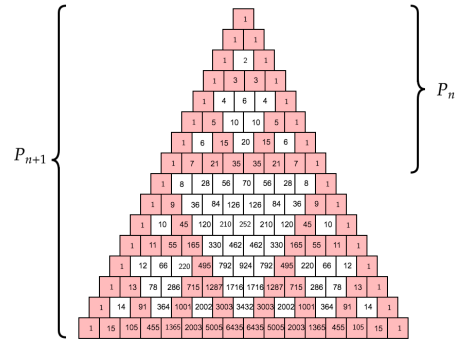


Figure 12: Pascals Triangle coloured red for odd values

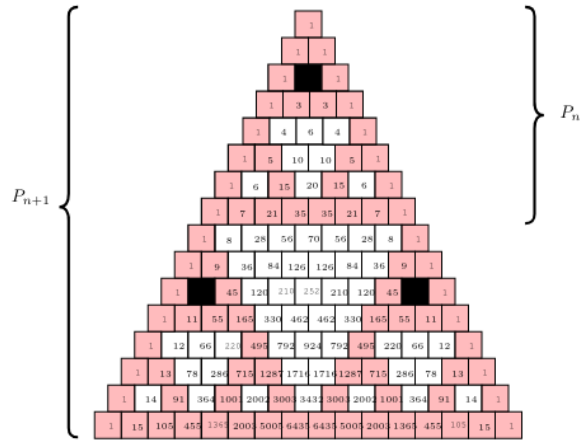


Figure 13: The black squares represent one example of a position on Pascal's triangle that are equivalent modulo 2

value modulo 2, at each corresponding row and column.

To prove this, we need to split the triangle into two parts, P_n denoting the first 2^n rows, i.e. the top “Sierpinski triangle” in Figure 12 and P_{n+1} representing the entire triangle. We must show that any chosen square in P_n is equal to the corresponding row and column in the lower two triangles of P_{n+1} , shown in Figure 13. This requires an identity that allows us to work with combinations in modulo 2, namely Lucas’ Theorem.

The connection Let $n, k \geq 0$ and for some prime p , we get:

$$\binom{n}{k} = \prod_{i=0}^m \binom{n_i}{k_i} \pmod{p} \quad (20)$$

where,

$$\begin{aligned} n &= n_m p^m + n_{m-1} p^{m-1} + \cdots + n_1 p + n_0, \\ k &= k_m p^m + k_{m-1} p^{m-1} + \cdots + k_1 p + k_0 \end{aligned}$$

are the expansions in radix p ¹⁵. This uses the convention that $\binom{n}{k} = 0$ if $k < n$

Take some arbitrary row r and column c in the triangle P_n . If we add 2^n rows to r , we will reach the equivalent row and column in the lower left triangle of P_{n+1} , since there are 2^n rows in P_n . In the same way, if we add 2^n columns to c we reach the equivalent row and column in the lower right triangle of P_{n+1} , leaving us with:

$$\begin{aligned} \text{Top Triangle: } & \binom{r}{c} \\ \text{Bottom-left Triangle: } & \binom{r + 2^n}{c} \\ \text{Bottom-right Triangle : } & \binom{r + 2^n}{c + 2^n} \end{aligned}$$

Using Lucas’ theorem, we can prove that the above statements are equivalent.

We can rewrite r and c in base 2 notation as follows:

$$\begin{aligned} r &= r_i 2^i + r_{i-1} 2^{i-1} + \cdots + r_1 2 + r_0 = [r_i r_{i-1} \cdots r_1 r_0]_2 \\ c &= c_i 2^i + c_{i-1} 2^{i-1} + \cdots + c_1 2 + c_0 = [c_i c_{i-1} \cdots c_1 c_0]_2 \end{aligned}$$

¹⁵Radix refers to a numerical system which uses some number of digits. Since we are working in modulo 2 for Pascal’s triangle, we are only concerned with the numbers 0 or 1, i.e. a radix 2 or a binary numeric system.

$$\begin{aligned}
\binom{2^n + r}{c} &\equiv \binom{1r_{i-1}r_{i-2}\cdots r_0}{0c_{i-1}c_{i-2}\cdots c_0} \pmod{2} \\
&\equiv \binom{1}{0} \binom{r_{i-1}}{c_{i-1}} \binom{r_{i-2}}{c_{i-2}} \cdots \binom{r_0}{c_0} \pmod{2} \\
&\equiv \binom{r_{i-1}}{c_{i-1}} \binom{r_{i-2}}{c_{i-2}} \cdots \binom{r_0}{c_0} \pmod{2} \\
&\equiv \binom{r}{c} \pmod{2}
\end{aligned}$$

$$\begin{aligned}
\binom{2^n + r}{2^n + c} &\equiv \binom{1r_{i-1}r_{i-2}\cdots r_0}{1c_{i-1}c_{i-2}\cdots c_0} \pmod{2} \\
&\equiv \binom{1}{1} \binom{r_{i-1}}{c_{i-1}} \binom{r_{i-2}}{c_{i-2}} \cdots \binom{r_0}{c_0} \pmod{2} \\
&\equiv \binom{r_{i-1}}{c_{i-1}} \binom{r_{i-2}}{c_{i-2}} \cdots \binom{r_0}{c_0} \pmod{2} \\
&\equiv \binom{r}{c} \pmod{2}
\end{aligned}$$

Thus, $\binom{r}{c} = \binom{2^n+r}{c} = \binom{2^n+r}{2^n+c} \pmod{2}$, which concludes the proof

2.5 Fractal Dimensions Sans Self Similarity

Not all fractals demonstrate obvious self-similarity, coastlines, as previously mentioned in §2.1, are a common example but are not unique in this regard, many natural phenomena such as the distribution of galaxies, shape of clouds, outline of mountains and the path of Brownian motion have a fractal structure [21, Ch. 2] that does not exhibit obvious self-similarity.

In order to measure the dimension of such fractals the log transformed measure and scale can be compared on a scatter plot in order to confirm that the relationship is linear, if the relationship is linear the dimension is constant and equal to the slope of the line, (see e.g. [59, §4.2], [53], mandelbrotHowLongCoast1967).

This approach is implemented to measure the dimension of the *Julia Set* in §5.4.

3 Connecting Fractals to Natural Processes

RYAN

In order to better understand the ways in which complex fractal patterns can emerge from simple processes, a simple process that leads to the emergence of such a pattern has been constructed, this is not a pattern that we have been able to find discussed in the literature but it does show simple connection between simple processes, patterns and the emergence of values such as golden ratio and the Fibonacci Sequence.

3.1 Constructing a Simple Process

Consider a fractal that begins simply with a square  , imagine that this square is replicated, rotated and appended  , then that shape, again is replicated rotated and appended  ,this process is illustrated in Figure 15, and if perpetuated a pattern emerges, as shown in Figure 14, this fractal can be generated by joining two matrices together in a manner that is consistent with the pattern described, this is shown in listing 6.

```

1 function matJoin(A, B)
2     function nrow(X)
3         return size(X)[1]
4     end
5     function ncol(X)
6         return size(X)[2]
7     end
8     emptymat = zeros(Bool, max(size(A)[1], size(B)[1]), sum(ncol(A) + ncol(B)) )
9     emptymat[1:nrow(A), 1:ncol(A)] = A
10    emptymat[1:nrow(B), (ncol(A)+1):ncol(emptymat)] = B
11    return emptymat
12 end
13
14 function mywalk(B, n)
15     for i in 1:n
16         B = matJoin(B, rotl90(B));
17     end
18     return B
19 end
20
21 GR.imshow(mywalk([1, 1], 9))

```

Listing 6: Generate the fractal described in §3 and shown in Figure 14

3.2 The Fibonacci Numbers

The fractal demonstrates a pattern that follows an angle that is caused by the join of the replicated and rotated unit ¹⁶, the shape of these joins is a rectangle that follows the Fibonacci numbers due to the additive nature of the process, this is illustrated in

¹⁶The term unit is used because this pattern would emerge whether or not squares were used, squares are merely more convenient because they relate to the box-counting measure and may be easily visualised.

3.2 The Fibonacci Numbers

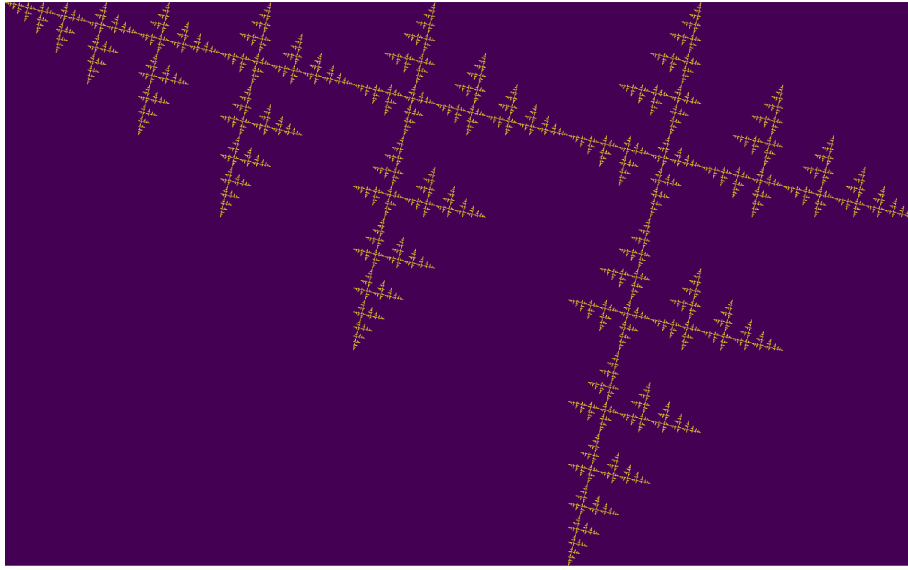


Figure 14: Fractal that emerges by Rotating and appending boxes, this demonstrates the relationship between the Fibonacci numbers and golden ratio very well

Figure 17, in §it is shown that $\lim \left(\frac{F_n}{F_{n-1}} \right) = \varphi$, this means that the edges of the fractal are proportional to one another as shown in listing 18 and so the angle can be given by the following relationship:

$$\theta = \tan^{-1} \left(\lim_{n \rightarrow \infty} \left(\frac{F_{n-2}}{F_n} \right) \right) \quad (21)$$

$$= \tan^{-1} \left(\lim_{n \rightarrow \infty} \left(\frac{F_{n-2}}{F_{n-1} + F_{n-2}} \right) \right) \quad (22)$$

$$= \tan^{-1} \left(\lim_{n \rightarrow \infty} \left(\frac{F_n}{F_{n+1} + F_n} \right) \right) \quad (23)$$

Because $\lim_{n \rightarrow \infty} \left(\frac{F_n}{F_{n-1}} \right) = \varphi \approx 1.618$ we can substite the values:

$$= \tan^{-1} (\varphi (\varphi + 1)) \quad (24)$$

$$= \tan^{-1} \left(\frac{\psi}{\varphi + 1} \right) \quad (25)$$

$$\approx 0.231^\circ \quad (26)$$

this is illustrated in Figures 17 and 18. This angle can be contrasted to the golden angle visualized in Figure 16 and although different it interesting to note that $2\pi \left(\frac{\psi}{\varphi+1} \right) \equiv 2\pi\psi \equiv 0 \pmod{\psi}$.

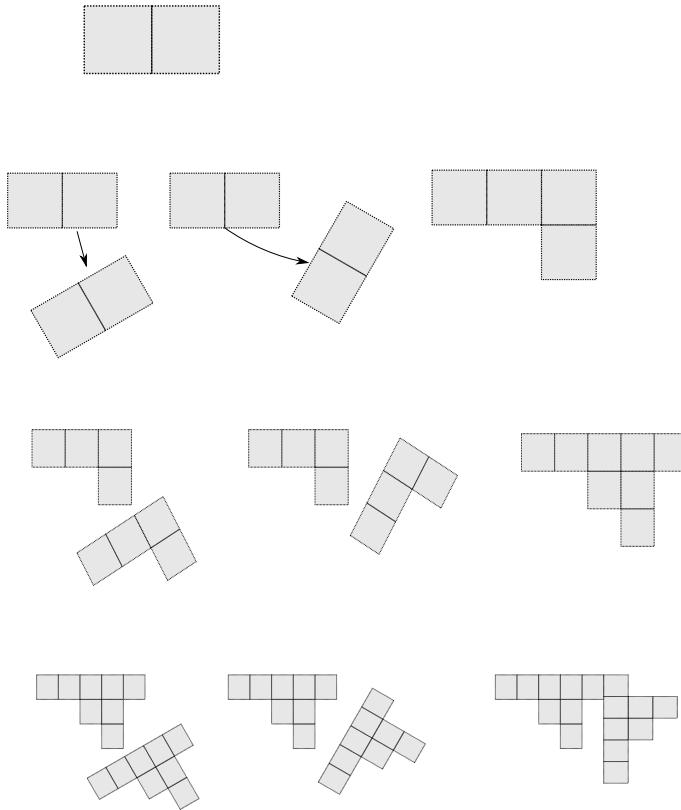


Figure 15: Process to generate the fractal shown in Figure 14 and described in 17. This process involves rotating and appending units and demonstrates a simple process from which the *Fibonacci Numbers* emerge from simple processes.

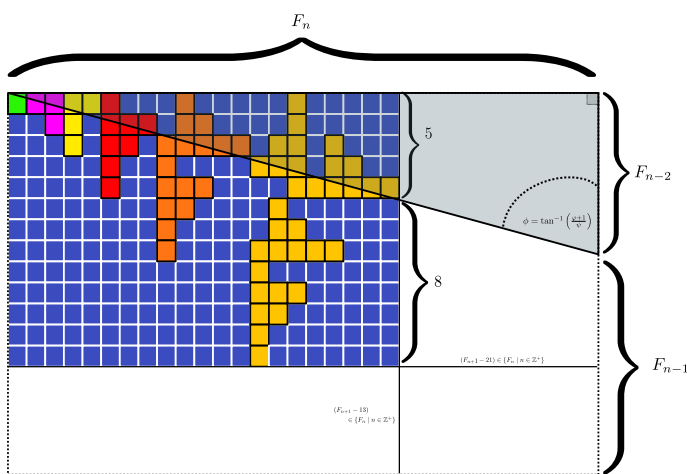


Figure 17: TODO

3.3 The Dimension of the Fractal

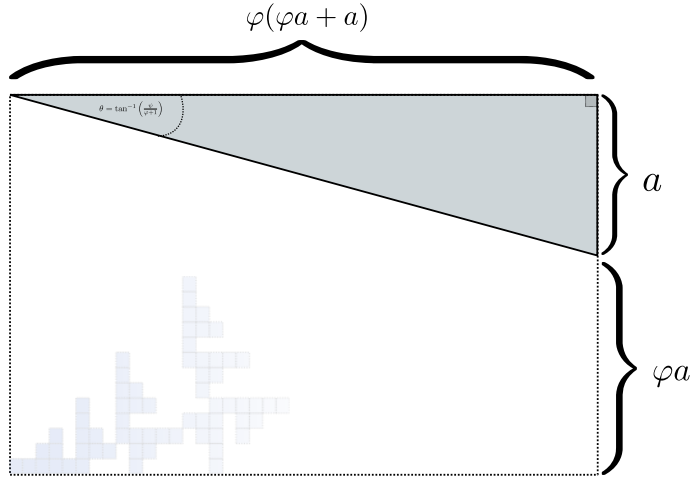


Figure 18: TODO

3.3 The Dimension of the Fractal

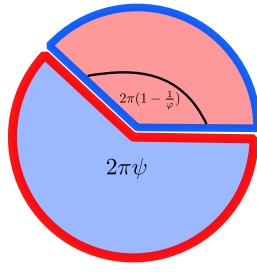


Figure 16: Diagram of the Golden Angle, an angle formed by having a ratio of edges equal to the golden ratio.

Each time this fractal is iterated the measure (i.e. the number of boxes) is doubled, but the scale of the fractal is increased by a ratio of the width and height, because the boxes add up this ratio will be a ratio of Fibonacci numbers which is shown to be equal to the golden ratio ϕ in §4, hence the dimension of this fractal is given by:

$$\log_\phi(2) = \frac{\log(2)}{\log(\phi)} \quad (27)$$

$$\approx 1.44042 \quad (28)$$

This value is consistent with measurements performed using *Julia* in listing 7.

4 The Fibonacci Sequence and the Golden Ratio

4.1 The Golden Ratio

RYAN

The *Fibonacci Sequence* and *Golden Ratio* occur in many patterns observed in natural phenomena (see [54, 3, 42, 44, 29, 52]), an example of such an occurrence is discussed in section 4.5 and a simple process demonstrating the emergence of the Fibonacci Numbers is discussed in §3.

The Golden Ratio is a value φ that satisfies the following property:

```

1  using DataFrames
2  function returnDim()
3      mat2 = mywalk(fill(1, 1, 1), 10)
4      l2   = sum(mat2)
5      size2 = size(mat2)[1]
6      mat1 = mywalk(fill(1, 1, 1), 11)
7      l1   = sum(mat1)
8      size1 = size(mat1)[1]
9      df = DataFrame()
10     df.measure = [log(l2/l1)/log(size2/size1)]
11     df.actual  = [log(2)/log(1.618) ]
12     return df
13 end
14
15 returnDim()
16
17 #-----
18
19 # 1x2 DataFrame
20 # | Row | measure | actual |
21 # |-----| Float64 | Float64 |
22 # | 1   | 1.44052 | 1.44048 |

```

Listing 7: Measure the fractal dimension of the fractal described in §3

$$\begin{aligned} \frac{a}{b} &= \frac{a+b}{a} = \varphi \\ \varphi &= 1 + \frac{1}{\varphi} \\ \implies \varphi^2 &= \varphi + 1 \end{aligned} \tag{29}$$

$$\implies \varphi = \frac{1 + \sqrt{5}}{2} \tag{30}$$

An interesting property of the golden ratio is that successive ratios of the Fibonacci numbers converge to the golden ratio.

Consider the series:

$$G_n = \frac{F_n}{F_{n-1}}$$

Such that F_n is the n^{th} Fibonacci Number:

$$F_n = F_{n-1} + F_{n-2}; \quad F_1 = F_2 = 1$$

4.2 Golden Ratio In terms of the Fibonacci Sequence

The Series G is alternating convergent series, to show that consider the two subsequences formed by taking the odd and even ratios, these are both bounded monotone sequences.

Since we are trying to show that the ratio of Fibonacci numbers converges by the Monotone Convergence Theorem, we will let G_n be as follows:

$$G_n = \left\{ \frac{F_{n+1}}{F_n} \right\}_{n=1}^{\infty}, \quad F_1 = F_2 = 1$$

To show G_n is bounded we must consider the following sub sequences,

1. $\{G_{2n}\}_{n=1}^{\infty}$ is bounded below and decreasing
2. $\{G_{2n-1}\}_{n=1}^{\infty}$ is bounded above and increasing

Proving (i):

To show $\{G_{2n}\}_{n=1}^{\infty}$ is decreasing we will show $G_{2n} - G_{2(n+1)} > 0$ through the process of induction.

Proof:

For least element $n = 1$:

$$\begin{aligned} G_2 - G_4 &= \frac{F_3}{F_2} - \frac{F_5}{F_4} \\ &= \frac{2}{1} - \frac{5}{3} \\ &> 0 \end{aligned}$$

Now assume true for all n :

$$G_{2n} - G_{2(n+1)} > 0 \implies \frac{G_{2n}}{G_{2(n+1)}} > 1$$

Prove true for $n + 1$:

$$\begin{aligned} G_{2(n+1)} - G_{2(n+2)} &= G_{2n+2} - G_{2n+4} \\ &= \frac{F_{2n+3}}{F_{2n+2}} - \frac{F_{2n+5}}{F_{2n+4}} \\ &= \frac{F_{2n+3}F_{2n+4} - F_{2n+5}F_{2n+2}}{F_{2n+2}F_{2n+4}} \\ &= \frac{F_{2n+3}(F_{2n+3} + F_{2n+2}) - F_{2n+2}(F_{2n+4} + F_{2n+3})}{F_{2n+2}F_{2n+4}} \\ &= \frac{(F_{2n+3})^2 - F_{2n+2}F_{2n+4}}{F_{2n+2}F_{2n+4}} \\ &= \frac{(F_{2n+3})^2}{F_{2n+2}F_{2n+4}} - 1 \\ &= \frac{F_{2n+3}}{F_{2n+2}} \cdot \frac{F_{2n+3}}{F_{2n+4}} - 1 \\ &= \frac{G_{2n+2}}{G_{2n+3}} - 1 \end{aligned}$$

Since $\frac{G_{2n}}{G_{2(n+1)}} > 1$ for all n by assumption, then $\frac{G_{2n+2}}{G_{2n+3}} > 1$ follows, hence

$$\begin{aligned} G_{2(n+1)} - G_{2(n+2)} &= \frac{G_{2n+2}}{G_{2n+3}} - 1 \\ &> 1 - 1 \\ &> 0 \end{aligned}$$

Therefore by mathematical induction, G_{2n} is monotonic decreasing.

Now, for $\{G_{2n}\}_{n=1}^{\infty}$ to be bounded below we will consider the entire set G_n , hence:

$$G_n = \frac{F_{n+1}}{F_n} = \frac{F_n + F_{n-1}}{F_n} = 1 + \frac{F_{n-1}}{F_n}$$

Since all Fibonacci numbers are positive, $\frac{F_{n-1}}{F_n} > 0$, so

$$G_n = 1 + \frac{F_{n-1}}{F_n} > 1$$

Thus G_n being bounded below implies G_{2n} is also bounded below.

Proving (ii):

To show $\{G_{2n}\}_{n=1}^{\infty}$ is decreasing we will show $G_{2n-1} - G_{2(n+1)-1} < 0$ through the process of induction.

Proof:

For least element $n = 1$:

$$\begin{aligned} G_1 - G_3 &= \frac{F_2}{F_1} - \frac{F_4}{F_3} \\ &= \frac{1}{1} - \frac{3}{2} \\ &< 0 \end{aligned}$$

Now assume true for all n :

$$G_{2n-1} - G_{2n+1} < 0 \implies \frac{G_{2n-1}}{G_{2n+1}} < 1$$

4.2 Golden Ratio In terms of the Fibonacci Sequence

Prove true for $n + 1$:

$$\begin{aligned}
 G_{2(n+1)-1} - G_{2(n+1)+1} &= G_{2n+1} - G_{2n+3} \\
 &= \frac{F_{2n+2}}{F_{2n+1}} - \frac{F_{2n+4}}{F_{2n+3}} \\
 &= \frac{F_{2n+2}F_{2n+3} - F_{2n+4}F_{2n+1}}{F_{2n+1}F_{2n+3}} \\
 &= \frac{F_{2n+2}(F_{2n+2} + F_{2n+1}) - F_{2n+1}(F_{2n+3} + F_{2n+2})}{F_{2n+1}F_{2n+3}} \\
 &= \frac{(F_{2n+2})^2 - F_{2n+1}F_{2n+3}}{F_{2n+1}F_{2n+3}} \\
 &= \frac{(F_{2n+2})^2}{F_{2n+1}F_{2n+3}} - 1 \\
 &= \frac{F_{2n+2}}{F_{2n+1}} \cdot \frac{F_{2n+2}}{F_{2n+3}} - 1 \\
 &= \frac{G_{2n+1}}{G_{2n+2}} - 1
 \end{aligned}$$

Since $\frac{G_{2n-1}}{G_{2n+1}} < 1$ for all n by assumption, then $\frac{G_{2n+1}}{G_{2n+2}} < 1$ follows, hence

$$\begin{aligned}
 G_{2(n+1)-1} - G_{2(n+1)+1} &= \frac{G_{2n+1}}{G_{2n+2}} - 1 \\
 &< 1 - 1 \\
 &< 0
 \end{aligned}$$

Therefore by mathematical induction, G_{2n-1} is increasing.

Now, for $\{G_{2n-1}\}_{n=1}^{\infty}$ to be bounded above we will again consider the entire set G_n , hence:

$$G_n = \frac{F_{n+1}}{F_n} = \frac{F_n + F_{n-1}}{F_n} = 1 + \frac{F_{n-1}}{F_n}$$

Since $\frac{F_{n-1}}{F_n} \leq 1$ we can deduce that

$$G_n = 1 + \frac{F_{n-1}}{F_n} \leq 2$$

Thus G_n being bounded above by 2 implies G_{2n-1} is also bounded above by 2.

4.2.2 Find the Limit

JAMES

By the Monotone Convergence Theorem, $\lim_{n \rightarrow \infty} G_n$ exists. We will assume that G_{2n} and G_{2n-1} approach the same limit $L \ \forall n \geq 1$ Meaning, we will also take:

$$\lim_{n \rightarrow \infty} G_n = \lim_{n \rightarrow \infty} G_{n-1} = L$$

$$\begin{aligned}\lim_{n \rightarrow \infty} G_n &= \lim_{n \rightarrow \infty} \frac{F_n + F_{n+1}}{F_{n+1}} \\&= 1 + \lim_{n \rightarrow \infty} \frac{F_{n-1}}{F_n} \\&= 1 + \lim_{n \rightarrow \infty} \frac{1}{G_{n-1}} \\&\implies L = 1 + \frac{1}{L} \\L^2 &= L + 1 \\0 &= L^2 - L - 1 \\&\implies L = \frac{\sqrt{5} + 1}{2} = \varphi\end{aligned}$$

4.3 Comments

RYAN

In the 13th century ¹⁷ Fibonacci developed ¹⁸ his namesake sequence when working on a problem concerning the growth rate of a rabbit population [52]. Continuous population growth is typically modelled with calculus by the equation $\frac{d}{dt}(p) \propto p$ [19, §11.1], what's interesting is that this population model itself generates a fractal when the number of stationary points is plotted against the growth rate [8, Ch. 3] and this fractal is equivalent to a plot of the Mandelbrot Set (discussed in §6) where the x -axis represents the real component of a value and the y -axis the number of iterations before a value exceeds a modulus of 2 (see generally [43]). This is not something we had time to investigate unfortunately but it does demonstrate the deep connection between natural phenomena such as population growth, the Fibonacci Sequence and complex fractals such as the Mandelbrot set.

4.3.1 Equivalent forms of the Golden Ratio

The golden ratio is sometimes expressed in odd forms in the literature:

$$\begin{aligned}\lim_{n \rightarrow \infty} \left[\frac{F_n}{F_{n-1}} \right] &= \varphi \\ \lim_{n \rightarrow \infty} \left[\frac{F_n}{F_{n-1}} \right] &= \psi \\ \varphi - \psi &= 1 \\ \varphi \times \psi &= 1 \\ \frac{\psi}{\varphi} &= \frac{1}{\varphi^2} = \frac{1}{1-\varphi} = \frac{1}{2-\varphi} = \frac{2}{3-\sqrt{5}}\end{aligned}$$

¹⁷Although strictly speaking this sequence can be traced back to 200 BC [49, 9]

¹⁸Or is it discovered?

4.4 A closed Solution for the Fibonacci Numbers

RYAN

The Fibonacci numbers can be solved using Calculus and this closed solution can be used to show that the ratio of Fibonacci numbers converges to the golden ratio.¹⁹

Consider the *Fibonacci Sequence*:

$$\begin{aligned} a_n &= a_{n-1} + a_{n-2} \\ \iff a_{n+2} &= a_{n+1} + a_n \end{aligned} \tag{31}$$

From observation, this appears similar in structure to the following *ordinary differential equation*, which would be fairly easy to deal with:

$$f''(x) - f'(x) - f(x) = 0$$

By ODE Theory we have $y \propto e^{m_i x}$, $i = 1, 2$ [66, §4.1.2] and the following power series [10, §64]:

$$f(x) = e^{mx} = \sum_{n=0}^{\infty} \left[r^m \frac{x^n}{n!} \right]$$

So using some sort of a transformation involving a power series may help to relate the discrete problem back to a continuous one.

Consider using the following generating function, (proof of the generating function derivative as in (33) and (34) is provided in section A.4)

$$f(x) = \sum_{n=0}^{\infty} \left[a_n \cdot \frac{x^n}{n!} \right] \tag{32}$$

$$\implies f'(x) = \sum_{n=0}^{\infty} \left[a_{n+1} \cdot \frac{x^n}{n!} \right] \tag{33}$$

$$\implies f''(x) = \sum_{n=0}^{\infty} \left[a_{n+2} \cdot \frac{x^n}{n!} \right] \tag{34}$$

So the Fibonacci recursive relation from (31) could be expressed :

$$\begin{aligned} a_{n+2} &= a_{n+1} + a_n \\ \frac{x^n}{n!} a_{n+2} &= \frac{x^n}{n!} (a_{n+1} + a_n) \\ \sum_{n=0}^{\infty} \left[\frac{x^n}{n!} a_{n+2} \right] &= \sum_{n=0}^{\infty} \left[\frac{x^n}{n!} a_{n+1} \right] + \sum_{n=0}^{\infty} \left[\frac{x^n}{n!} a_n \right] \end{aligned}$$

¹⁹For further material related to exponential generating function see A.4 of the appendix.

And hence by applying (32), (33) and (34):

$$f''(x) = f'(x) + f(x) \quad (35)$$

Using the theory of higher order linear differential equations with constant coefficients it can be shown:

$$f(x) = c_1 \cdot \exp\left[\left(\frac{1-\sqrt{5}}{2}\right)x\right] + c_2 \cdot \exp\left[\left(\frac{1+\sqrt{5}}{2}\right)x\right]$$

By equating this to the power series:

$$f(x) = \sum_{n=0}^{\infty} \left[\left(c_1 \left(\frac{1-\sqrt{5}}{2}\right)^n + c_2 \left(\frac{1+\sqrt{5}}{2}\right)^n\right) \cdot \frac{x^n}{n!} \right]$$

Now given that:

$$f(x) = \sum_{n=0}^{\infty} \left[a_n \frac{x^n}{n!} \right]$$

We can conclude that:

$$a_n = c_1 \cdot \left(\frac{1-\sqrt{5}}{2}\right)^n + c_2 \cdot \left(\frac{1+\sqrt{5}}{2}\right)^n$$

By applying the initial conditions:

$$\begin{aligned} a_0 &= c_1 + c_2 \implies c_1 = -c_2 \\ a_1 &= c_1 \left(\frac{1+\sqrt{5}}{2}\right) - c_1 \left(\frac{1-\sqrt{5}}{2}\right) \implies c_1 = \frac{1}{\sqrt{5}} \\ &\therefore c_1 = \frac{1}{\sqrt{5}}, c_2 = -\frac{1}{\sqrt{5}} \end{aligned}$$

And so finally we have the solution to the *Fibonacci Sequence* 31:

$$\begin{aligned} a_n &= \frac{1}{\sqrt{5}} \left[\left(\frac{1+\sqrt{5}}{2}\right)^n - \left(\frac{1-\sqrt{5}}{2}\right)^n \right] \\ &= \frac{\varphi^n - \psi^n}{\sqrt{5}} \\ &= \frac{\varphi^n - \psi^n}{\varphi - \psi} \end{aligned} \quad (36)$$

where:

- $\varphi = \frac{1+\sqrt{5}}{2} \approx 1.61\dots$
- $\psi = 1 - \varphi = \frac{1-\sqrt{5}}{2} \approx 0.61\dots$

4.4.1 Golden Ratio

This closed solution (36) also demonstrates that successive terms of the Fibonacci numbers converge to the Golden Ratio:

$$\begin{aligned} F_n &= \frac{\varphi^n - \psi^n}{\varphi - \psi} = \frac{\varphi^n - \psi^n}{\sqrt{5}} \\ \iff \frac{F_{n+1}}{F_n} &= \frac{\varphi^{n+1} - \psi^{n+1}}{\varphi^n - \psi^n} \\ \iff \lim_{n \rightarrow \infty} \left[\frac{F_{n+1}}{F_n} \right] &= \lim_{n \rightarrow \infty} \left[\frac{\varphi^{n+1} - \psi^{n+1}}{\varphi^n - \psi^n} \right] \\ &= \frac{\varphi^{n+1} - \lim_{n \rightarrow \infty} [\psi^{n+1}]}{\varphi^n - \lim_{n \rightarrow \infty} [\psi^n]} \end{aligned}$$

because $|\psi| < 0$ $n \rightarrow \infty \implies \psi^n \rightarrow 0$:

$$\begin{aligned} &= \frac{\varphi^{n+1} - 0}{\varphi^n - 0} \\ &= \varphi \end{aligned}$$

4.5 Sunflower Seeds; Fibonacci Numbers in Nature



Figure 19: Distribution of the seeds of a sunflower [7]

not been reviewed, rather a simple approach to model this phenomena in a way that can be easily programmed with Turtle Graphics (implemented also in §2.4.2) has been devised,

Assume that the process a sunflower follows when placing seeds is as follows:²⁰

1. Place a seed

The distribution of sunflower seeds is an example of the *Fibonacci Sequence* occurring in a pattern observed in nature (see Figure 19), the distribution of seeds produces a spiral pattern and the number of clockwise and anti-clockwise spirals that emerge tend to be Fibonacci Numbers. [5]

Although the emergence of the Fibonacci Numbers with respect to the sunflower head and models to explain this emergence is well documented in the literature (see e.g. [51, 40, 60]) these have

²⁰To clarify, this process is merely conjecture, other than seeing a very nice example at MathIsFun.com [44], no evidence is presented to suggest that this is the way that sunflowers distribute their seeds.

However the simulations performed within *Julia* are very encouraging and suggest that this process may offer good insight into the underlying mechanisms.

2. Move some small unit away from the origin
3. Rotate some constant angle θ from the previous seed (with respect to the origin).
4. Repeat this process until a seed hits some outer boundary.

This process can be simulated in Julia as shown in listing 8 . When a variety of different angles of rotation are tried varrious different patterns emerge, such patterns are shown in Figure 21, choosing an angle of φ produces output as shown in Figure 21.

A distribution of seeds under this process would be optimal if the amount of empty space was minimised, spirals, stars and swirls contain patterns that compromise this.

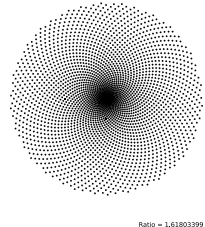


Figure 20: Optimisation of simulated distribution of Sunflower seeds occurs for $\theta = 2\varphi\pi$ as described in section 4.5 and listing 8

To minimize this, the proportion of the circle traversed in step 3 must be an irrational number, however this alone is not sufficient, the decimal values must also be not to approximated by a rational number, for example [44]:

- $\pi \bmod 1 \approx \frac{1}{7} = 0.71428571428$
- $e \bmod 1 \approx \frac{5}{7} = 0.142857142857$

It can be seen by simulation that ϕ and ψ (because $\phi \bmod 1 = \psi$) are solutions to this optimisation problem as shown in Figure 20, this solution is unstable, a very minor change to the value will result in patterns re-emerging in the distribution.²¹

The bottom right spiral in Figure 21 has a ratio of rotation of $\frac{1}{\pi}$, the spirals look similar to one direction of the spirals occurring in Figure 20, it is not clear if there is any significance to this similarity.

5 Julia Sets

RYAN

5.1 Introduction

Julia sets provide an example of a family of very complex structures that emerge from a very simple mathematical processes.

²¹An early goal of this project was to demonstrate that $\theta = \varphi$ had the greatest number of seeds, ideally this would have been implemented using a box-counting method but difficulties in applying this were encountered and so this was not undertaken.

5.1 Introduction

```

1  φ = 1.61803398875
2  ψ = φ^-1
3  Ψ = 0.61803398875
4  function sfSeeds(ratio)
5    a = Turtle()
6    for θ in [(ratio*2*π)*i for i in 1:3000]
7      gsave()
8      scale(0.05)
9      rotate(θ)
10     #      Pencolor([], rand(1)[1], rand(1)[1], rand(1)[1])
11
12     Forward(a, 1)
13     Rectangle(a, 50, 50)
14     grestore()
15   end
16   label = string("Ratio = ", round(ratio, digits = 8))
17   textcentered(label, 100, 200)
18 end
19 @svg begin
20   sfSeeds(φ)
21 end 600 600

```

Listing 8: Simulation of the distribution of sunflowers as described in section 4.5

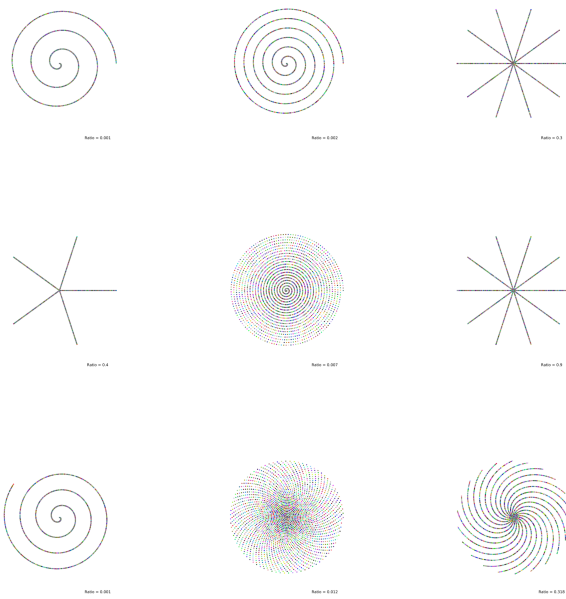


Figure 21: Simulated Distribution of Sunflower seeds as described in section 4.5 and listing 8

5.2 Motivation

Consider the iterative process $x \rightarrow x^2$, $x \in \mathbb{R}$, for values of $x > 1$ this process will diverge and for $x < 1$ it will converge.

The iterative process $z \rightarrow z^2$, $z \in \mathbb{C}$, for values of $|z| > 1$ diverges and for $|z| < 1$ it will converge, this is visualized in 23

This can be generalised, consider:

- The complex plane for $|z| \leq 1$
- Some function $f_c(z) = z^2 + c$, $c \leq 1 \in \mathbb{C}$ that can be used to iterate with

Every value on that plane will belong to one of the two following sets

- P_c
 - The set of values on the plane that converge to zero (prisoners)
 - Define $Q_c^{(k)}$ to be the the set of values confirmed as prisoners after k iterations of f_c
 - * this implies $\lim_{k \rightarrow \infty} [Q_c^{(k)}] = P_c$
- E_c
 - The set of values on the plane that tend to ∞ (escapees)

In the case of $f_0(z) = z^2$ all values $|z| \leq 1$ are bounded with $|z| = 1$ being an unstable stationary circle, but for different iterative functions like $f_1(z) = z^2 - 1$ the circle of convergence distorts to a fractal pattern, the set of all points on the boundary of convergence is said to be the *Julia Set* [47, Ch. 14].

5.3 Plotting the Sets

To implement this test we'll consider a function called `escape_test` that applies an iteration (in this case $f_0 : z \rightarrow z^2$) until that value diverges or converges.²²

While iterating with f_c once $|z| > \max(\{|c|\}, 2)$, the value must diverge because $|c| \leq 1$, so rather than record whether or not the value converges or diverges, the `escape_test` can instead record the number of iterations (k) until the value has crossed that boundary and this will provide a measurement of the rate of divergence.

The `escape_test` function can then be mapped over a matrix, where each element of that matrix is in turn mapped to a point on the Cartesian Plane, the resulting matrix can be visualised as an image, this is implemented in listing 10 and the corresponding output shown in 23.

Observe that the absolute value was not used in 10 (or below in §5.4), this is because a `sqrt` is a costly operation that can be avoided by comparing two squares, this is important when multiple iterations over large matrices are required, this accounted for as much as 50% of the time required to generate the data using listing 2.1 in §5.4.

²²This technique was adapted from Chapter 7 of *Math adventures with Python* [16]

5.3 Plotting the Sets

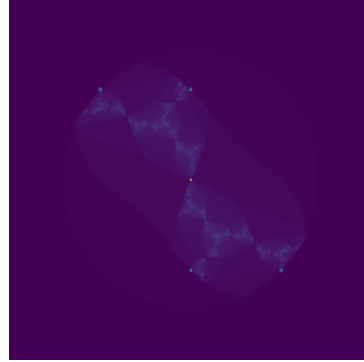


Figure 22: Circle of Convergence for $f_0 : z \rightarrow z^2 - 1$

```

1   from math import sqrt
2   def magnitude(z):
3       # return sqrt(z[0]**2 + z[1]**2)
4       x = z[0]
5       y = z[1]
6       return sqrt(sum(map(lambda x: x**2, [x, y])))
7
8   def cAdd(a, b):
9       x = a[0] + b[0]
10      y = a[1] + b[1]
11      return [x, y]
12
13
14  def cMult(u, v):
15      x = u[0]*v[0]-u[1]*v[1]
16      y = u[1]*v[0]+u[0]*v[1]
17      return [x, y]

```

Listing 9: Defining Complex Operations with vectors

The resulting circle in Figure 23 is precisely what would be expected, verifying this approach. Consider now the result if this same procedure was applied to a slightly different function, for example the following functions:

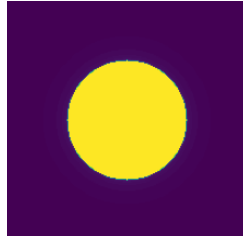


Figure 23: Circle of Convergence for $f_0 : z \rightarrow z^2$

$$f_{\frac{1}{4}+\frac{i}{2}} : z \rightarrow z^2 + \left(\frac{1}{4} + \frac{i}{2}\right)$$

The result is remarkably unexpected, as shown in Figures 22 and 24.

To investigate this further consider the more general function:

$$f_{0.8e^{\pi i\tau}} : z \rightarrow z^2 + 0.8e^{\pi i\tau}, \quad \tau \in \mathbb{R} \quad (37)$$

```

1 %matplotlib inline
2 %config InlineBackend.figure_format = 'svg'
3 import numpy as np
4 def escape_test(z, num):
5     ''' runs the process num amount of times and returns the count of
6     divergence'''
7     c = [0, 0]
8     count = 0
9     z1 = z #Remember the original value that we are working with
10    # Iterate num times
11    while count <= num:
12        dist = sum([n**2 for n in z1])
13        distc = sum([n**2 for n in c])
14        # check for divergence
15        if dist > max(2, distc):
16            #return the step it diverged on
17            return count
18        #iterate z
19        z1 = cAdd(cMult(z1, z1), c)
20        count+=1
21        #if z hasn't diverged by the end
22
23
24
25
26 p = 0.25 #horizontal, vertical, pinch (zoom)
27 res = 200
28 h = res/2
29 v = res/2
30
31 pic = np.zeros([res, res])
32 for i in range(pic.shape[0]):
33     for j in range(pic.shape[1]):
34         x = (j - h)/(p*res)
35         y = (i-v)/(p*res)
36         z = [x, y]
37         col = escape_test(z, 100)
38         pic[i, j] = col
39
40 import matplotlib.pyplot as plt
41
42 plt.axis('off')
43
44 plt.imshow(pic)
# plt.show()

```

Listing 10: Circle of Convergence of z under recursion

5.4 Dimension of the Julia Set

Many fractals can be generated using this set by varying the value of τ^{23} . *Julia* will be used to implement this due to performance constraints. These images can be generated in *Julia* in a similar fashion as before, with the specifics shown in listing 11. The GR package appears to be the best plotting library performance wise and so was used to save corresponding images to disc, this is demonstrated in listing 12 where 1200 pictures at a 2.25 MP resolution were produced.²⁴

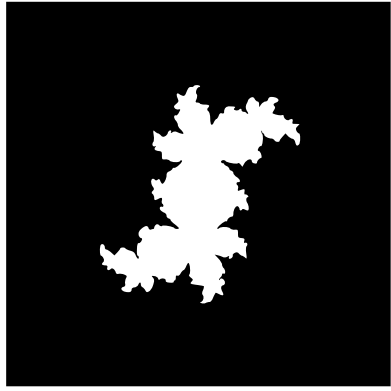


Figure 24: Boundary of Convergence for $f_{\frac{1}{4} + \frac{i}{2}} : z \rightarrow z^2 + \frac{1}{4} + \frac{i}{2}$, the figure was contrasted using *ImageMagick* to highlight the complex boundary

A subset of these images can be combined using *ImageMagick* and bash to create a collage, *ImageMagick* can also be used to produce an animation but it often fails and a superior approach is to use *ffmpeg*, this is demonstrated in listing 13, the collage is shown in Figure 25.

5.4 Dimension of the Julia Set

The Julia Set is defined as the boundary between which values diverge and converge on the complex plane [14, §14.1], this means a matrix representing such a fractal must only have values along this boundary. This can be achieved by looping over every element of a matrix and replacing each value with 0 if it is surrounded on all sides values.

To implement this for a boolean matrix a function could consider if immediately adjacent elements sum to 9, that point should be set to 0 if this is true because it does not represent a boundary. This is implemented in 14 and although this will not perfectly trace the outline of a fractal like the *Julia Set*, it is expected that this approach will not introduce bias and so the impact on accuracy will be constant for *Julia Sets* across all scales of resolution.

In order to measure the dimension of the *Julia Set* it is necessary to generate a representation of the fractal at two scales, compare them and then measure the corresponding dimension value as in §2.4. The julia set is a non self-similar fractal and so it is not immediately clear whether or not the dimension will be constant at all scales, to determine whether or not the dimension is constant at various scales it can be convenient to plot the log transformed scaling factor and measures and inspect whether or not the points form a linear relationship, the slope of such a relationship will be the dimension as discussed in §2.5.

To implement this all the functions necessary to build the fractals were placed into a separate script `julia-set-functions.jl` which is shown in § and this script

²³This approach was inspired by an animation on the *Julia Set* Wikipedia article [25]

²⁴This took about 30 minutes on an Intel I7-7700 with 32GB memory using *Julia* 1.5.2

```

1  # * Define the Julia Set
2  """
3  Determine whether or not a value will converge under iteration
4  """
5  function juliaSet(z, num, my_func)
6      count = 1
7      # Remember the value of z
8      z1 = z
9      # Iterate num times
10     while count ≤ num
11         # check for divergence
12         if abs(z1)>2
13             return Int(count)
14         end
15         #iterate z
16         z1 = my_func(z1) # + z
17         count=count+1
18     end
19     #if z hasn't diverged by the end
20     return Int(num)
21 end
22
23 # * Make a Picture
24 """
25 Loop over a matrix and apply apply the julia-set function to
the corresponding complex value
26 """
27 function make_picture(width, height, my_func)
28     pic_mat = zeros(width, height)
29     zoom = 0.3
30     for i in 1:size(pic_mat)[1]
31         for j in 1:size(pic_mat)[2]
32             x = (j-width/2)/(width*zoom)
33             y = (i-height/2)/(height*zoom)
34             pic_mat[i,j] = juliaSet(x+y*im, 256, my_func)
35         end
36     end
37     return pic_mat
38 end
39

```

Listing 11: Produce a series of fractals using julia

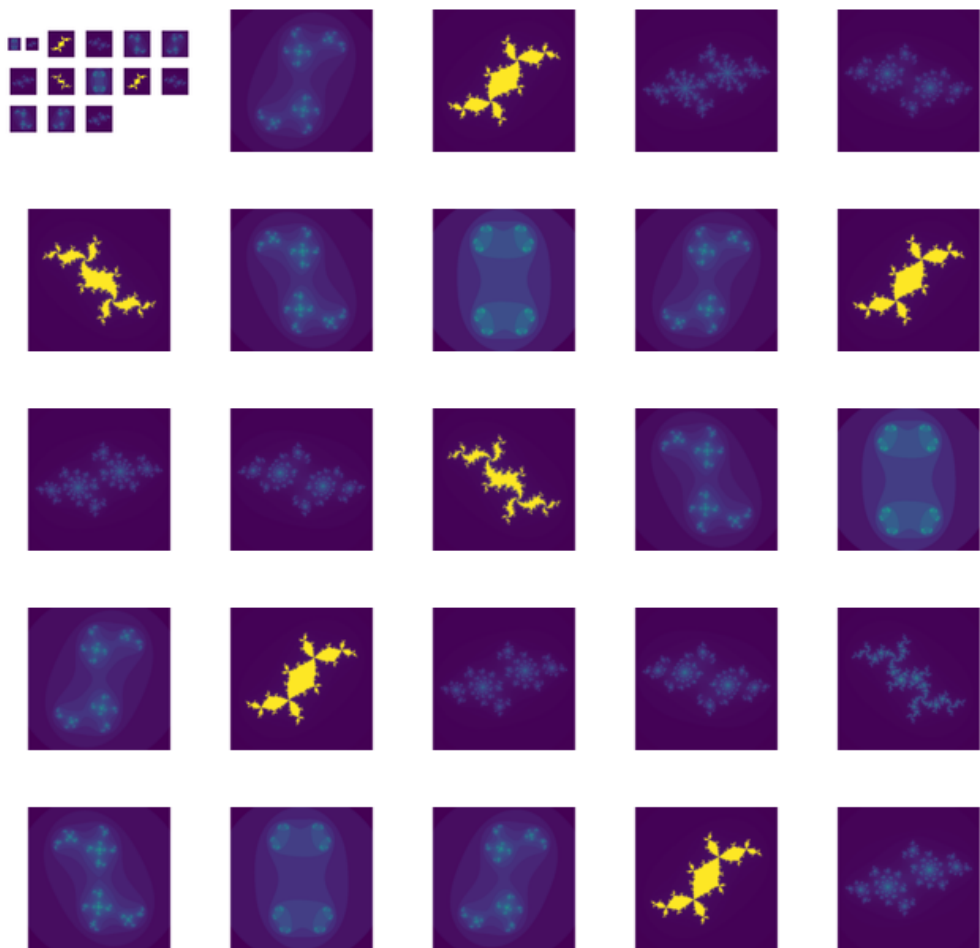
5.4 Dimension of the Julia Set

```
1 # * Use GR to Save many images
2     ## GR is faster than PyPlot
3 using GR
4 function save_images(count, res)
5     try
6         mkdir("/tmp/gifs")
7     catch
8     end
9     j = 1
10    for i in (1:count)/(40*2*pi)
11        j = j + 1
12        GR.imshow(make_picture(res, res, z -> z^2 + 0.8*exp(i*im*9/2))) # PyPlot uses
13        ↪ interpolation = "None"
14        name = string("/tmp/gifs/j", lpad(j, 5, "0"), ".png")
15        GR.savefig(name)
16    end
17 end
18 save_images(1200, 1500) # Number and Res
```

Listing 12: Generate and save the images with GR

```
1 # Use montage multiple times to get recursion for fun
2 montage (ls *.png | sed -n '1p;0~600p') 0a.png
3 montage (ls *.png | sed -n '1p;0~100p') a.png
4 montage (ls *.png | sed -n '1p;0~50p') -geometry 1000x1000 a.png
5
6 # Use ImageMagick to Produce a gif (unreliable)
7 convert -delay 10 *.png 0.gif
8
9 # Use FFmpeg to produce a Gif instead
10 ffmpeg
11     -framerate 60
12     -pattern_type glob
13     -i '*.png'
14     -r 15
15     out.mov
```

Listing 13: Using bash, ffmpeg and *ImageMagick* to combine the images and produce an animation.

Figure 25: Various fractals corresponding to $f_{0.8e^{\pi i \tau}}$

5.4 Dimension of the Julia Set

```
1  function outline(mat)
2      work_mat = copy(mat)
3      for col in 2:(size(mat)[2]-1)
4          for row in 2:(size(mat)[1]-1)
5              ## Make the inside 0, we only want the outline
6              neighbourhood = mat[row-1:row+1,col-1:col+1]
7              if sum(neighbourhood) >= 9 # 9 squares
8                  work_mat[row,col] = 0
9              end
10         end
11     end
12     return work_mat
13 end
```

Listing 14: A function to set all values of matrix, that do not represent the boundary of a shape, to zero. This is designed for a boolean matrix and works by summing the neighbourhood of an element, if that neighbourhood is greater than 9 (indicating that all values surrounding the point contain an element), the value is set to 1.

was included into a working script `julia-set-dimensions.jl` by using the following line:

```
1  @time include("./Julia-Set-Dimensions-functions.jl")
```

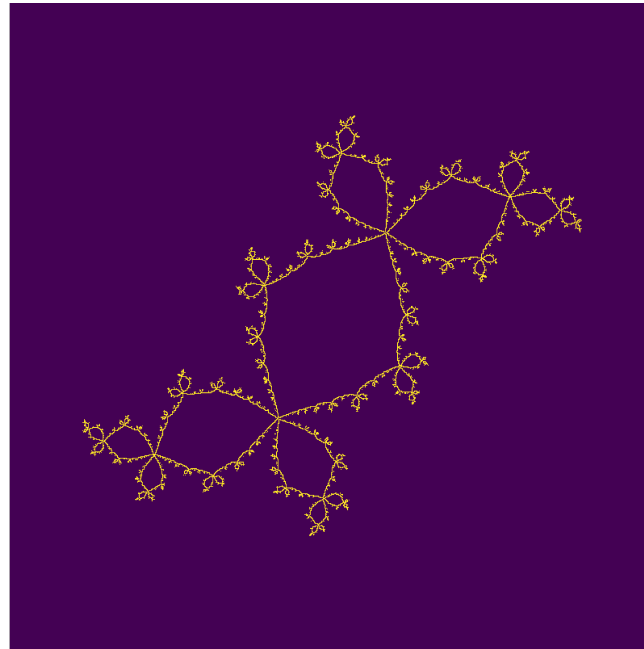


Figure 26: Image of the Douady Rabbit, the julia set corresponding to the iteration of $z \leftarrow z^2 - 0.123 + 0.745i$ produced by *Julia* in listing 15.

The working script to measure the dimension of the Julia Set is shown in listing 15. This script generates fractals of the *Julia Set* corresponding to $z \leftarrow z^2 - 0.123 + 0.745i$ for a variety of different scales, at each scale the measure of the fractal is recorded and by running the code in listing 15 for scales from 9000 to 10000 and leaving it for an hour, the following table of values is returned:

<i>Scale</i>	<i>Mass</i>
500	4834.0
563	5754.0
625	6640.0
688	7584.0
750	8418.0
813	9550.0
875	10554.0
938	11710.0
1000	12744.0

Using this technique the dimension of the Julia Set converges very slowly and the code can take a very long time to run, and has a tendency to cause crashes, likely due to the large amounts of memory required, the values produced took about one hour to produce.

Linear Regression can be performed against these values using **R**²⁵

²⁵The could just as well have been done inside Julia, **R** was chosen simply because `ggplot` produces

5.4 Dimension of the Julia Set

```

1  @time include("./Julia-Set-Dimensions-functions.jl")
2
3  ##### Investigate Plot #####
4  test_mat = make_picture(800,800, z -> z^2 + -0.123+0.745*im)
5
6  #Inspect
7  GR.imshow(test_mat) # PyPlot uses interpolation = "None"
8  # Outline
9  test_mat = outline(test_mat)
10 #Inspect
11 GR.imshow(test_mat) # PyPlot uses interpolation = "None"
12 ## Return the perimeter
13 sum(test_mat)
14
15 # Take a measurement at a point
16 mat2 = outline(make_picture(9000,9000, f))
17 l2 = sum(mat2)
18 size2 = size(mat2)[1]
19 mat1 = outline(make_picture(10000,10000, f))
20 l1 = sum(mat1)
21 size1 = size(mat1)[1]
22 log(l2/l1)/log(size2/size1)
23 # 1.3934 Douady Rabbit
24
25 # Take a measurement using LInear Regression
26 using CSV
27 @time data=scaleAndMeasure(900, 1000 , 4, f)
28 # CSV.read("./julia-set-dimensions.csv", data)
29 # data = CSV.read("./julia-set-dimensions.csv")
30 data.scale = [log(i) for i in data.scale]
31 data.mass = [log(i) for i in data.mass]
32 mod = lm(@formula(mass ~ scale), data)

33 p = Gadfly.plot(data, x=:scale, y=:mass, Geom.point)
34
35 print("the slope is $(round(coef(mod)[2], sigdigits=4))")
36 print(mod)
37 print("\n")
38 return mod
39
40 a = SharedArray{Float64}(10)
41 @distributed for i = 1:10
42     a[i] = i
43 end
44
45 #-----
46 # julia> return mod
47 #
48 # mass ~ θ + scale
49 #
50 # Coefficients:
51 # _____
52 #      Coef.   Std. Error          t  Pr(>|t|)  Lower 95%  Upper 95%
53 # _____
54 # scale  1.28358  0.000497296  2581.11      <1e-9    1.28199    1.28516
55 # _____

```

Listing 15: Functions used by listing 15

```

1 scale <- c(500, 563, 625, 688, 750, 813, 875, 938, 1000)
2 measure <- c( 4834, 5754, 6640, 7584, 8418, 9550, 10554, 11710, 12744)
3 data <- data.frame(scale, measure)
4
5 lm(log(measure) ~ 0 + log(scale), data)$coefficients # set 0 intercept
6
7 #-----#
8 # 1.36720041333112

```

This shows that the value returned is 1.37 which is very close to the value of 1.39 which is reported in the literature [41]. A plot can be produced (shown in Figure 27) by using the following **R** code:

```

1 library(ggplot2)
2 ggplot(data, aes(x = log(measure), y = log(scale))) +
3   geom_point(size = 6, col = 'red') +
4   geom_smooth(method = 'lm') +
5   theme_bw() +
6   labs(x = "log Measure", y = "log Scale",
7        title = "Comparison of Scale and Measure of Julia Set", subtitle = "Douady Rabbit")
8

```

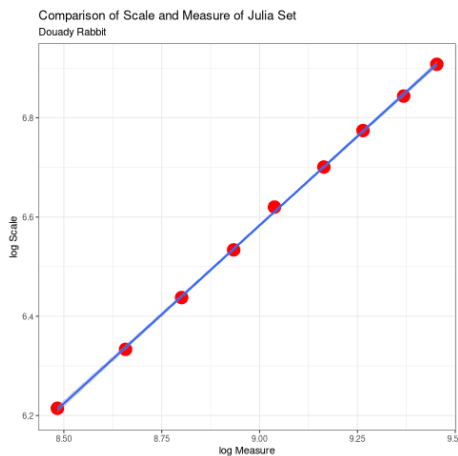


Figure 27: Log Scaled Linear Regression of various scales of the julia set.

Inspecting the behaviour of the log transformed scale and measure in Figure 27 indicates that there is a very linear relationship between these variables and so even though this julia set does not appear to demonstrate simple self-similarity, it appears to be a figure with a constant dimension across scales.

very nice plots.

6 Mandelbrot Set

RYAN

Investigating the Julia Set in Figure 25, a natural question arises, *which values of c produce a fractal that is an open disc or a closed disc*. If an arbitrary complex value $|\gamma| < 1$ is chosen to produce the julia set f_γ , that value is said to belong to the Mandelbrot set if the corresponding *Julia Set* is a closed disc [47, Ch. 14]. P is closed we this value is defined as belonging to the *Mandelbrot set*.

It can be shown, that a value z_0 is interior to the *Mandelbrot Set* if f_{z_0} is interior to the julia set and hence this problem is equivalent to re-implementing the previous strategy such that $z \rightarrow z^2 + z_0$ where z_0 is unchanging or more clearly as a sequence:

$$z_{n+1} = z_n^2 + c \quad (38)$$

$$z_0 = c \quad (39)$$

This strategy is implemented in listing and produces the output shown in Figure 28.

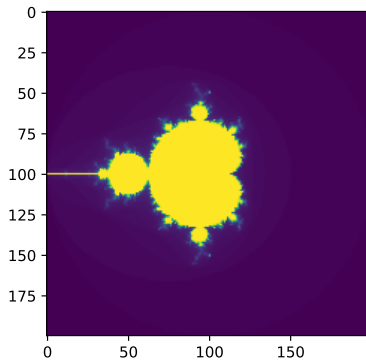


Figure 28: Mandelbrot Set produced in *Python* as shown in listing 16

This output although remarkable is however fairly undetailed, by using *Julia* a much larger image can be produced, in *Julia* producing a 4 GB, 400 MP image can be done in little time (about 10 minutes on my system), this is demonstrated in listing 17 and a screenshot of the corresponding FITS image is shown in listing 29.

```

1  %matplotlib inline
2  %config InlineBackend.figure_format = 'svg'
3  import numpy as np
4
5  def mandelbrot(z, num):
6      """ runs the process num amount of times and returns the count of
7          divergence"""
8      count = 0
9      # Define z1 as z
10     z1 = z
11     # Iterate num times
12     while count <= num:
13         # check for divergence
14         if magnitude(z1) > 2.0:
15             #return the step it diverged on
16             return count
17         #iterate z
18         z1 = cAdd(cMult(z1, z1),z)
19         count+=1
20         #if z hasn't diverged by the end
21     return num
22
23 p = 0.25 # horizontal, vertical, pinch (zoom)
24 res = 200
25 h = res/2
26 v = res/2
27
28 pic = np.zeros([res, res])
29 for i in range(pic.shape[0]):
30     for j in range(pic.shape[1]):
31         x = (j - h)/(p*res)
32         y = (i-v)/(p*res)
33         z = [x, y]
34         col = mandelbrot(z, 100)
35         pic[i, j] = col
36
37 import matplotlib.pyplot as plt
38 plt.imshow(pic)
39 # plt.show()

```

Listing 16: All values of c that lead to a closed Julia-set

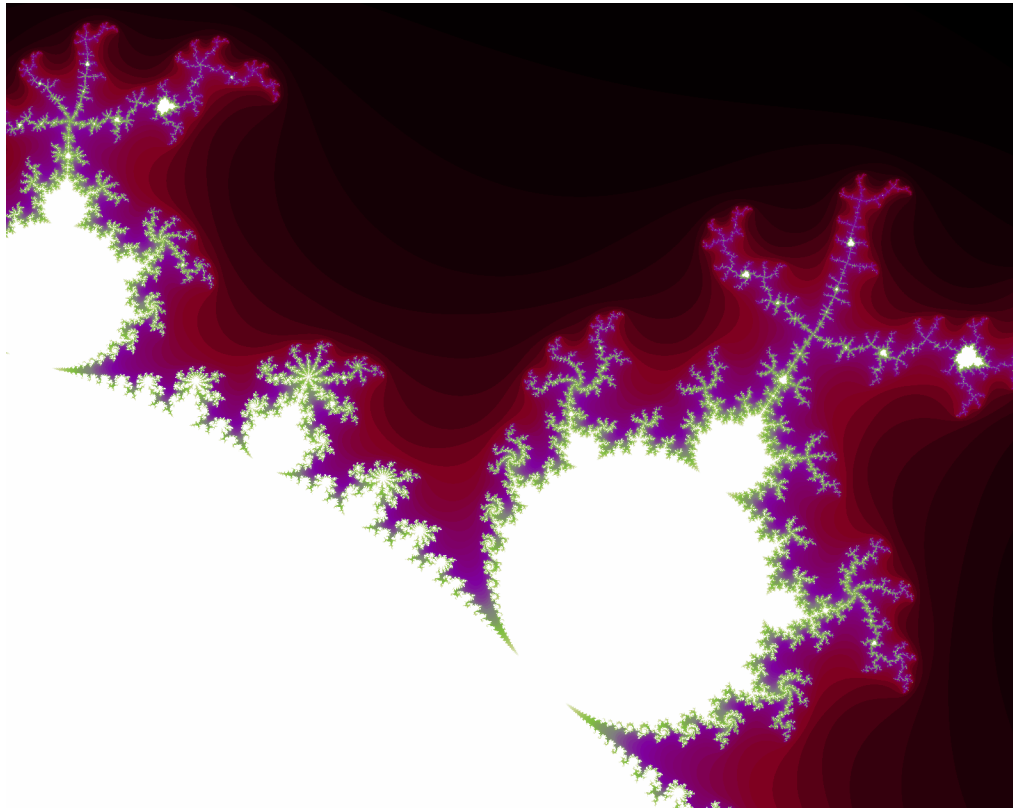


Figure 29: Screenshot of Mandelbrot FITS image produced by listing 17

The dimension of the mandelbrot set is 2 [6] and can be measured using the exact same strategy as §5.4.²⁶ The Mandelbrot set is extraordinarily complex and actually contains many of the patterns of various Julia Sets within it [47, Ch. 14].

7 Conclusion

RYAN

Fractals are complex shapes that may or may not exhibit self similarity and often arise from natural phenomena. They are hard to define in a way that captures all potential edge cases. One important feature of fractals is the dimension of the complex shape, they are not simple finite shapes and so their dimension is usually higher than what might be anticipated by considering the corresponding dimension of a shape that may approximate the general figure.

This concept of dimension can be extended to shapes that do not exhibit clear self-similarity by using linear regression, this includes particularly complex fractals such as the Mandelbrot Set.

²⁶As a matter of fact it would only be necessary to uncomment the end of line 40 of the listing provided in §A.3 and use the function `juliaSet(z, z -> z^2)`

```

1  function mandelbrot(z, num, my_func)
2      count = 1
3      # Define z1 as z
4      z1 = z
5      # Iterate num times
6      while count ≤ num
7          # check for divergence
8          if abs(z1)>2
9              return Int(count)
10         end
11         #iterate z
12         z1 = my_func(z1) + z
13         count=count+1
14     end
15     #if z hasn't diverged by the end
16     return Int(num)
17 end
18
19 function make_picture(width, height, my_func)
20     pic_mat = zeros(width, height)
21     for i in 1:size(pic_mat)[1]
22         for j in 1:size(pic_mat)[2]
23             x = j/width
24             y = i/height
25             pic_mat[i,j] = mandelbrot(x+y*im, 99, my_func)
26         end
27     end
28     return pic_mat
29 end
30
31
32 using FITSIO
33 function save_picture(filename, matrix)
34     f = FITS(filename, "w");
35     # data = reshape(1:100, 5, 20)
36     # data = pic_mat
37     write(f, matrix) # Write a new image extension with the data
38
39     data = Dict("col1"=>[1., 2., 3.], "col2"=>[1, 2, 3]);
40     write(f, data) # write a new binary table to a new extension
41
42     close(f)
43 end
44
45 # * Save Picture
46 #-----
47 my_pic = make_picture(20000, 20000, z -> z^2) 2000^2 is 4 GB
48 save_picture("/tmp/a.fits", my_pic)

```

Listing 17: Generate High Resolution Mandelbrot Set and Export as Fits Image using Julia.

Simple processes that involve recursion can lead to the emergence of patterns that are fractals, these fractals can often include other characteristic properties that involve values such as the golden ratio and Fibonacci Numbers.

A Appendix

So unless code contributes directly to the discussion we'll put it in the appendix.

A.1 Code Listings

The code listings used to produce Sierpinski's Carpet and Cantor's Dust are provided in listings 18 and 19 respectively.

```
1 #-----
2 #-- Function -----
3 #
4
5 function carpet(ICMat, width)
6     B = ICMat
7     h = size(B)[1]
8     w = size(B)[2]
9     Z = zeros(Int, h, w)
10    B = [B B B;
11          B Z B;
12          B B B]
13    if (3*w) < width
14        B = carpet(B, width)
15    end
16    return B
17 end
18 #
19 #-----#
20 #-- Plot -----
21 #
22 using GR, Plots
23 gr() # Set Plots backend as GR
24
25 (mat = carpet(fill(1, 1, 1), 9^2)) |> size
26 p1 = GR.imshow(mat)
27
28 #
29 #-- Dimension -----
30 #
31 mat2 = carpet(fill(1, 1, 1), 1000)
32 l2 = sum(mat2)
33 size2 = size(mat2)[1]
34 mat1 = carpet(fill(1, 1, 1), 500)
35 l1 = sum(mat1)
36 size1 = size(mat1)[1]
37
38 #
39 ## julia> log(l2/l1)/log(size2/size1)
40 ## 1.89
```

Listing 18: Function to produce Sierpinski's carpet, shown in Figure 2.4.1

```

1  #-----
2  #--- Function -----
3  #-----
4
5  function dust(ICMat, width)
6      B = ICMat
7      h  = size(B)[1]
8      w  = size(B)[2]
9      Z  = zeros(Int, h, w)
10     B = [Z Z B Z;
11          B Z Z Z;
12          Z Z Z B;
13          Z B Z Z]
14     if (3*w)<width
15         B = dust(B, width)
16     end
17     return B
18 end
19
20 #-----
21 #--- Plot -----
22 #-----
23 using GR, Plots
24 gr() # Set Plots backend as GR
25
26 (mat = dust(fill(1, 1, 1), 9^2)) |> size
27 p1 = GR.imshow(mat)
28
29
30 #-----
31 #--- Dimension -----
32 #-----
33 mat2 = dust(fill(1, 1, 1), 1000)
34 l2  = sum(mat2)
35 size2 = size(mat2)[1]
36 mat1 = dust(fill(1, 1, 1), 500)
37 l1  = sum(mat1)
38 size1 = size(mat1)[1]
39
40 #-----
41 ## julia> log(l2/l1)/log(size2/size1)
42 ## 1.0

```

Listing 19: Function to generate Cantor Dust, shown in

A.2 Resources Used for the Hausdorff Dimension

Research for §on the Hausdorff Dimension proved actually to be quite difficult, while much information is available online, precice and clear explanations of the Hausdorff dimension are difficult to find without scouring texts, the following proved very helpful generally in preparing for this topic and I would strongly recommend these chapters as a starting point for further reading on this topic:

- Edgar, G. A., *Measure, topology, and fractal geometry* [12, Ch. 6]
- Falconer, K. J., *Fractal geometry: mathematical foundations and applications* [14, Ch. 2]

A.3 Functions for constructing the Julia Set

- Gouyet, J., *Physics and fractal structures* [21, §1.3]
- Vicsek, T., *Fractal Growth Phenomena* [59, Ch. 4]
 - See also p 14 specifically
- Tél, T., Gruiz, M., & Kulacsy, K., *Chaotic dynamics: an introduction based on classical mechanics* [57, §2.1.2]
- Peitgen, H., Jürgens, H., & Saupe, D., *Chaos and fractals: new frontiers of science* [47, §4.3]

A.3 Functions for constructing the Julia Set

The following functions were saved in a file called:

- `@time include("./Julia-Set-Dimensions-functions.jl")`

This file was loaded into the current workspace by using the following at the top of a *Julia* script:

- `@time include("./Julia-Set-Dimensions-functions.jl")`

```
1  using GR
2  using DataFrames
3  using Gadfly
4  using GLM
5  using SharedArrays
6  using Distributed
7
8  #####
9  ### Julia / MandelBrot Functions #####
10 #####
11 """
12
13 # Julia Set
14 Returns how many iterations it takes for a value on the complex plane to diverge
15 under recursion. if `boolQ` is specified as true a 1/0 will be returned to
16 indicate divergence or convergence.
17
18 ## Variables
19 - `z`
20   - A value on the complex plane within the unit circle
21 - `num`
22   - A number of iterations to perform before conceding that the value is not
23     divergent.
24 - `my_func`
25   - A function to perform on `z`, for a julia set the function will be of the
26     form `z -> z^2 + a + im*b`
27   - So for example the Douady Rabbit would be described by `z -> z^2 -0.123+0.745*im`
28 """
29 function juliaSet(z, num, my_func, boolQ=true)
30   count = 1
31   # Define z1 as z
32   z1 = z
33   # Iterate num times
34   while count ≤ num
35     # check for divergence
```

A APPENDIX

```
36     if real(z1)^2+imag(z1)^2 > 2^2
37         if(boolQ) return 0 else return Int(count) end
38     end
39     #iterate z
40     z1 = my_func(z1) # + z
41     count=count+1
42 end
43     #if z hasn't diverged by the end
44     if(boolQ) return 1 else return Int(count) end
45 end
46
47 """
48 # Mandelbrot Set
49 Returns how many iterations it takes for a value on the complex plane to diverge
50 under recursion of  $\text{z} \rightarrow z^2 + z_0$ .
51
52 Values that converge represent constants of the julia set that lead to a
53 connected set. (TODO: Have I got that Vice Versa?)
54
55
56 ## Variables
57 - `z`
58   - A value on the complex plane within the unit circle
59 - `num`
60   - A number of iterations to perform before conceding that the value is not
61     divergent.
62 - `boolQ`
63   - `true` or `false` value indicating whether or not to return 1/0 values
64     indicating divergence or convergence respectively or to return the number of
65     iterations performed before conceding no divergence.
66 """
67 function mandelbrot(z, num, boolQ = true)
68     count = 1
69     # Define z1 as z
70     z1 = z
71     # Iterate num times
72     while count ≤ num
73         # check for divergence
74         if real(z1)^2+imag(z1)^2 > 2^2
75             if(boolQ) return 0 else return Int(count) end
76         end
77         #iterate z
78         z1 = z1^2 + z
79         count=count+1
80     end
81     #if z hasn't diverged by the end
82     return 1 # Int(num)
83     if(boolQ) return 1 else return Int(count) end
84 end
85
86
87 function test(x, y)
88     if(x<1) return x else return y end
89 end
90
91 #####
92 ##### Build a Matrix Image #####
93 #####
94 #####
95 """
96
97 # Make a Picture
98
99 This maps a function on the complex plane to a matrix where each element of the
```

A.3 Functions for constructing the Julia Set

```
100 matrix corresponds to a single value on the complex plane. The matrix can be
101 interpreted as a greyscale image.
102
103 Inside the function is a `zoom` parameter that can be modified for different
104 fractals, fur the julia and mandelbrot sets this shouldn't need to be adjusted.
105
106 The height and width should be interpreted as resolution of the image.
107
108 - `width`
109   - width of the output matrix
110 - `height`
111   - height of the output matrix
112 - `myfunc`
113   - Complex Function to apply across the complex plane
114 """
115 function make_picture(width, height, my_func)
116   pic_mat = zeros(width, height)
117   zoom = 0.3
118   for j in 1:size(pic_mat)[2]
119     for i in 1:size(pic_mat)[1]
120       x = (j-width/2)/(width*zoom)
121       y = (i-height/2)/(height*zoom)
122       pic_mat[i,j] = juliaSet(x+y*im, 256, my_func)
123     end
124   end
125   return pic_mat
126 end
127
128 ##### Make the Outline #####
129 ### Make the Outline #####
130 #####
131 """
132
133 # Outline
134
135 Sets all elements with neighbours on all sides to 0.
136
137 - `mat`
138   - A matrix
139   - If this matrix is the convergent values corresponding to a julia set the
140     output will be the outline, which is the definition of the julia set.
141 """
142 function outline(mat)
143   work_mat = copy(mat)
144   for col in 2:(size(mat)[2]-1)
145     for row in 2:(size(mat)[1]-1)
146       ## Make the inside 0, we only want the outline
147       neighbourhood = mat[row-1:row+1,col-1:col+1]
148       if sum(neighbourhood) >= 9 # 9 squares
149         work_mat[row,col] = 0
150       end
151     end
152   end
153   return work_mat
154 end
155
156
157 ##### Return many Scaled Values #####
158 #####
159 #####
160
161
162
163 function scaleAndMeasure(min, max, n, func)
```

```

164 # The scale is equivalent to the resolution, the initial resolution could be
165 # set as 10, 93, 72 or 1, it's arbitrary (previously I had res and scale)
166 # #TODO: Prove this
167
168 scale = [Int(ceil(i)) for i in range(min, max, length=n) ]
169 mass = pmmap(s -> sum(outline(make_picture(Int(s), Int(s), func))) , scale)
170
171 data = DataFrame(scale = scale, mass = mass)
172 return data
173
end

```

A.4 Exponential Generating Functions

Exponential Generating Functions can be used to find solutions to linear recurrence relations, Markov Chains and Differential Equations and may provide insight into the connections between discrete and continuous process.

We were unable to find time to show generally the relationship between homogeneous ODEs and homogenous linear recurrence relations and this work was not directly relevant to this report, it is included in this appendix for reference sake.

Derivative of the Exponential Generating Function

BaseRYAN Differentiating the exponential generating function has the effect of shifting the sequence once to the left: [31]

$$f(x) = \sum_{n=0}^{\infty} \left[a_n \frac{x^n}{n!} \right] \quad (40)$$

$$\begin{aligned} f'(x) &= \frac{d}{dx} \left(\sum_{n=0}^{\infty} \left[a_n \frac{x^n}{n!} \right] \right) \\ &= \frac{d}{dx} \left(a_0 \frac{x^0}{0!} + a_1 \frac{x^1}{1!} + a_2 \frac{x^2}{2!} + a_3 \frac{x^3}{3!} + \dots \frac{x^k}{k!} \right) \\ &= \sum_{n=0}^{\infty} \left[\frac{d}{dx} \left(a_n \frac{x^n}{n!} \right) \right] \\ &= \sum_{n=0}^{\infty} \left[\frac{a_n}{(n-1)!} x^{n-1} \right] \\ \implies f'(x) &= \sum_{n=1}^{\infty} \left[\frac{x^n}{n!} a_{n+1} \right] \quad (41) \end{aligned}$$

Bridge JAMES This can be shown for all derivatives by way of induction, for

$$f^{(k)}(x) = \sum_{n=k}^{\infty} \frac{a_{n+k} \cdot x^n}{n!} \quad \text{for } k \geq 0 \quad (42)$$

A.4 Exponential Generating Functions

Assume that $f^{(k)}(x) = \sum_{n=k}^{\infty} \frac{a_{n+k} \cdot x^n}{n!}$

Using this assumption, prove for the next element $k + 1$

We need $f^{(k+1)}(x) = \sum_{n=k+1}^{\infty} \frac{a_{n+k+1} \cdot x^n}{n!}$

$$\begin{aligned}
\text{LHS} &= f^{(k+1)}(x) \\
&= \frac{d}{dx} (f^{(k)}(x)) \\
&= \frac{d}{dx} \left(\sum_{n=k}^{\infty} \frac{a_{n+k} \cdot x^n}{n!} \right) \quad \text{by assumption} \\
&= \sum_{n=k}^{\infty} \frac{a_{n+k} \cdot n \cdot x^{n-1}}{n!} \\
&= \sum_{n=k}^{\infty} \frac{a_{n+k} \cdot x^{n-1}}{(n-1)!} \\
&= \sum_{n=k+1}^{\infty} \frac{a_{n+k+1} \cdot x^n}{n!} \\
&= \text{RHS}
\end{aligned}$$

Therefore, by mathematical induction $f^{(k)}(x) = \sum_{n=k}^{\infty} \frac{a_{n+k} \cdot x^n}{n!}$ for $k \geq 0$

Furthermore, if the first derivative of the exponential generating function shown in (41) shifts the sequence across, then every derivative thereafter does so as well.

Homogeneous Proof

RYAN:JAMES An equation of the form:

$$\sum_{i=0}^n [c_i \cdot f^{(i)}(x)] = 0 \tag{43}$$

is said to be a homogenous linear ODE: [64, Ch. 2]

Linear because the equation is linear with respect to $f(x)$

Ordinary because there are no partial derivatives (e.g. $\frac{\partial}{\partial x}(f(x))$)

Differential because the derivates of the function are concerned

Homogenous because the **RHS** is 0

- A non-homogeneous equation would have a non-zero RHS

There will be k solutions to a k^{th} order linear ODE, each may be summed to produce a superposition which will also be a solution to the equation, [64, Ch. 4] this will be considered as the desired complete solution (and this will be shown to be the only solution for the recurrence relation (44)). These k solutions will be in one of two forms:

1. $f(x) = c_i \cdot e^{m_i x}$

A APPENDIX

2. $f(x) = c_i \cdot x^j \cdot e^{m_i x}$

where:

- $\sum_{i=0}^k [c_i m^{k-i}] = 0$
 - This is referred to as the characteristic equation of the recurrence relation or ODE [32]
- $\exists i, j \in \mathbb{Z}^+ \cap [0, k]$
 - These are often referred to as repeated roots [32, 65] with a multiplicity corresponding to the number of repetitions of that root [45, §3.2]

Unique Roots of Characteristic Equation RYAN An example of a recurrence relation with all unique roots is the fibonacci sequence, as described in section 4.4.

1. Proof Consider the linear recurrence relation (44):

$$\sum_{i=0}^n [c_i \cdot a_i] = 0, \quad \exists c \in \mathbb{R}, \quad \forall i < k \in \mathbb{Z}^+$$

This implies:

$$\sum_{n=0}^{\infty} \left[\sum_{i=0}^k \left[\frac{x^n}{n!} c_i a_n \right] \right] = 0 \quad (44)$$

$$\sum_{n=0}^{\infty} \sum_{i=0}^k \frac{x^n}{n!} c_i a_n = 0 \quad (45)$$

$$\sum_{i=0}^k c_i \sum_{n=0}^{\infty} \frac{x^n}{n!} a_n = 0 \quad (46)$$

By implementing the exponential generating function as shown in (32), this provides:

$$\sum_{i=0}^k \left[c_i f^{(i)}(x) \right] \quad (47)$$

Now assume that the solution exists and all roots of the characteristic polynomial are unique (i.e. the solution is of the form $f(x) \propto e^{m_i x} : m_i \neq m_j \forall i \neq j$), this implies that [64, Ch. 4] :

$$f(x) = \sum_{i=0}^k [k_i e^{m_i x}], \quad \exists m, k \in \mathbb{C}$$

A.4 Exponential Generating Functions

This can be re-expressed in terms of the exponential power series, in order to relate the solution of the function $f(x)$ back to a solution of the sequence a_n , (see section for a derivation of the exponential power series

$$\begin{aligned}
 \sum_{i=0}^k [k_i e^{m_i x}] &= \sum_{i=0}^k \left[k_i \sum_{n=0}^{\infty} \frac{(m_i x)^n}{n!} \right] \\
 &= \sum_{i=0}^k \sum_{n=0}^{\infty} k_i m_i^n \frac{x^n}{n!} \\
 &= \sum_{n=0}^{\infty} \sum_{i=0}^k k_i m_i^n \frac{x^n}{n!} \\
 &= \sum_{n=0}^{\infty} \left[\frac{x^n}{n!} \sum_{i=0}^k [k_i m_i^n] \right], \quad \exists k_i \in \mathbb{C}, \quad \forall i \in \mathbb{Z}^+ \cap [1, k]
 \end{aligned} \tag{48}$$

Recall the definition of the generating function from (32), by equating this to (48):

$$\begin{aligned}
 f(x) &= \sum_{n=0}^{\infty} \left[\frac{x^n}{n!} a_n \right] \\
 &= \sum_{n=0}^{\infty} \left[\frac{x^n}{n!} \sum_{i=0}^k [k_i m_i^n] \right] \\
 \implies a_n &= \sum_{i=0}^k [k_i m_i^n]
 \end{aligned}$$

□

This can be verified by the fibonacci sequence as shown in section 4.4, the solution to the characteristic equation is $m_1 = \varphi, m_2 = (1 - \varphi)$ and the corresponding solution to the linear ODE and recursive relation are:

$$\begin{aligned}
 f(x) &= c_1 e^{\varphi x} + c_2 e^{(1-\varphi)x}, \quad \exists c_1, c_2 \in \mathbb{R} \subset \mathbb{C} \\
 \iff a_n &= k_1 n^\varphi + k_2 n^{1-\varphi}, \quad \exists k_1, k_2 \in \mathbb{R} \subset \mathbb{C}
 \end{aligned}$$

Repeated Roots of Characteristic Equation

RYAN

- Example Consider the following recurrence relation:

$$\begin{aligned}
 a_{n+2} - 10a_{n+1} + 25a_n &= 0 \tag{49} \\
 \implies \sum_{n=0}^{\infty} \left[a_{n+2} \frac{x^n}{n!} \right] - 10 \sum_{n=0}^{\infty} \left[a_{n+1} \frac{x^n}{n!} \right] + 25 \sum_{n=0}^{\infty} \left[a_n \frac{x^n}{n!} \right] &= 0
 \end{aligned}$$

By applying the definition of the exponential generating function at (32) :

$$f''(x) - 10f'(x) + 25f(x) = 0 \quad (50)$$

By implementing the already well-established theory of linear ODE's, the characteristic equation for (50) can be expressed as:

$$\begin{aligned} m^2 - 10m + 25 &= 0 \\ (m - 5)^2 &= 0 \\ m &= 5 \end{aligned} \quad (51)$$

Herein lies a complexity, in order to solve this, the solution produced from (51) can be used with the *Reduction of Order* technique to produce a solution that will be of the form [65, §4.3].

$$f(x) = c_1 e^{5x} + c_2 x e^{5x} \quad (52)$$

(52) can be expressed in terms of the exponential power series in order to try and relate the solution for the function back to the generating function, observe however the following power series identity ²⁷ (proof in section):

$$x^k e^x = \sum_{n=k}^{\infty} \left[\frac{x^n}{(n-k)!} \right], \quad \exists k \in \mathbb{Z}^+ \quad (53)$$

by applying identity (53) to equation (52)

$$\begin{aligned} \implies f(x) &= \sum_{n=0}^{\infty} \left[c_1 \frac{(5x)^n}{n!} \right] + \sum_{n=1}^{\infty} \left[c_2 n \frac{(5x)^n}{n(n-1)!} \right] \\ &= \sum_{n=0}^{\infty} \left[\frac{x^n}{n!} (c_1 5^n + c_2 n 5^n) \right] \end{aligned}$$

Given the defenition of the exponential generating function from (32)

²⁷This identity is something that was conjectured to exist by Ryan by making connections between the recurrence relations and ODE's, establishing that this identity was actually true however was shown by James.

$$f(x) = \sum_{n=0}^{\infty} \left[a_n \frac{x^n}{n!} \right]$$

$$\iff a_n = c_1 5^n + c_2 5^n$$

□

2. Proof Consider a recurrence relation of the form:

$$\begin{aligned} \sum_{n=0}^k [c_i a_n] &= 0 \\ \implies \sum_{n=0}^{\infty} \sum_{i=0}^k c_i a_n \frac{x^n}{n!} &= 0 \\ \sum_{i=0}^k \sum_{n=0}^{\infty} c_i a_n \frac{x^n}{n!} & \end{aligned}$$

By substituting for the value of the generating function from (32):

$$\sum_{i=0}^k [c_i f^{(k)}(x)] \tag{54}$$

Assume that (54) corresponds to a characteristic polynomial with only 1 root of multiplicity k , the solution would hence be of the form:

$$\begin{aligned} \sum_{i=0}^k [c_i m^i] &= 0 \wedge m = B, \quad \exists! B \in \mathbb{C} \\ \implies f(x) &= \sum_{i=0}^k [x^i A_i e^{mx}], \quad \exists A \in \mathbb{C}^+, \quad \forall i \in [1, k] \cap \mathbb{N} \end{aligned} \tag{55}$$

By implementing the identity first introduced at (53) (this is proved in §):

$$x^k e^x = \sum_{n=k}^{\infty} \left[\frac{x^n}{(n-k)!} \right] \tag{56}$$

See section for proof.

We can apply identity (53) to (55), which gives:

$$\begin{aligned}
f(x) &= \sum_{i=0}^k \left[A_i \sum_{n=i}^{\infty} \left[\frac{(xm)^n}{(n-i)!} \right] \right] \\
&= \sum_{n=0}^{\infty} \left[\sum_{i=0}^k \left[\frac{x^n}{n!} \frac{n!}{(n-i)!} A_i m^n \right] \right] \\
&= \sum_{n=0}^{\infty} \left[\frac{x^n}{n!} \sum_{i=0}^k \left[\frac{n!}{(n-i)!} A_i m^n \right] \right]
\end{aligned}$$

Recall the generating function that was used to get (54):

$$\begin{aligned}
f(x) &= \sum_{n=0}^{\infty} \left[a_n \frac{x^n}{n!} \right] \\
\implies a_n &= \sum_{i=0}^k \left[A_i \frac{n!}{(n-i)!} m^n \right] \\
&= \sum_{i=0}^k \left[m^n A_i \prod_0^k [n - (i-1)] \right] \\
&\quad \because i \leq k \\
&= \sum_{i=0}^k \left[A_i^* m^n n^i \right], \quad \exists A_i \in \mathbb{C}, \quad \forall i \leq k \in \mathbb{Z}^+
\end{aligned} \tag{57}$$

□

3. Power Series Identity for Products of Exponentials In this section a proof for identity ?? is provided.

(a) Motivation

JAMES

Consider the function $f(x) = xe^x$. Using the taylor series formula we get the following:

$$\begin{aligned}
xe^x &= 0 + \frac{1}{1!}x + \frac{2}{2!}x^2 + \frac{3}{3!}x^3 + \frac{4}{4!}x^4 + \frac{5}{5!}x^5 + \dots \\
&= \sum_{n=0}^{\infty} \frac{nx^n}{n!} \\
&= \sum_{n=1}^{\infty} \frac{x^n}{(n-1)!}
\end{aligned}$$

A.4 Exponential Generating Functions

Similarly, $f(x) = x^2 e^x$ will give:

$$\begin{aligned} x^2 e^x &= \frac{0}{0!} + \frac{0x}{1!} + \frac{2x^2}{2!} + \frac{6x^3}{3!} + \frac{12x^4}{4!} + \frac{20x^5}{5!} + \dots \\ &= \frac{2 \cdot 1x^2}{2!} + \frac{3 \cdot 2x^3}{3!} + \frac{4 \cdot 3x^4}{4!} + \frac{5 \cdot 4x^5}{5!} + \dots \\ &= \sum_{n=2}^{\infty} \frac{n(n-1)x^n}{n!} \\ &= \sum_{n=2}^{\infty} \frac{x^n}{(n-2)!} \end{aligned}$$

We conjecture that If we continue this on, we get:

$$x^k e^x = \sum_{n=k}^{\infty} \frac{x^n}{(n-k)!} \quad \text{for } k \in \mathbb{Z}^+ \cap 0$$

- (b) Proof by Induction JAMES To verify, let's prove this by induction.
- i. Base Test $k = 0$

$$\begin{aligned} LHS &= x^0 e^x = e^x \\ RHS &= \sum_{n=0}^{\infty} \frac{x^n}{n!} = e^x \end{aligned}$$

- Therefore LHS = RHS, so $k = 0$ is true
- ii. Bridge Assume $x^k e^x = \sum_{n=k}^{\infty} \frac{x^n}{(n-k)!}$
Using this assumption, prove for the next element $k+1$

We need $x^{k+1} e^x = \sum_{n=k+1}^{\infty} \frac{x^n}{(n-(k+1))!}$

$$\begin{aligned} LHS &= x^{k+1} e^x \\ &= x \cdot x^k e^x \\ &= x \cdot \sum_{n=k}^{\infty} \frac{x^n}{(n-k)!} \quad (\text{by assumption}) \\ &= \sum_{n=k}^{\infty} \frac{x^{n+1}}{(n-k)!} \\ &= \sum_{n=k+1}^{\infty} \frac{x^n}{(n-1-k)!} \quad (\text{re-indexing } n) \\ &= \sum_{n=k+1}^{\infty} \frac{x^n}{(n-(k+1))!} \\ &= RHS \end{aligned}$$

A APPENDIX

So by mathematical induction $f(x) = x^k e^x = \sum_{n=k}^{\infty} \frac{x^n}{(n-k)!}$ for $k \geq 0$
 Moving on, by applying identity (53) to equation (52)

- (c) Establishing the Proof RYAN We make the assumption that
 $(x)! = \Gamma(x) \forall x \in \mathbb{R}$, If it can be shown that $\frac{1}{\Gamma(x)} = 0 \ \forall x \in \mathbb{R} < 0$ then observe the following:

$$\sum_{n=0}^{k-1} \left[\frac{x^n}{(n-x)!} \right] = \sum_{n=0}^{k-1} \left[\frac{1}{\Gamma(n-k)} \cdot x^n \right] \quad (58)$$

because $n - k < 0 \ \forall n \in [0, n-k]$

:

$$= \sum_{n=0}^{k-1} [0 \times x^n] \quad (59)$$

$$= 0 \quad (60)$$

and hence:

$$\sum_{n=0}^{\infty} \left[\frac{x^n}{(n-x)!} \right] = \sum_{n=0}^{k-1} \left[\frac{x^n}{\Gamma(n-x)} \right] + \sum_{n=k}^{\infty} \left[\frac{x^n}{(n-x)!} \right] \quad (61)$$

$$= 0 + \sum_{n=k}^{\infty} \left[\frac{x^n}{(n-x)!} \right] \quad (62)$$

From the inductive proof before:

$$= x^k e^x \quad (63)$$

- (d) Divergence of the Gamma Function

JAMES

$$\Gamma(-p) = \int_0^{\infty} t^{-p-1} e^{-t} dt \quad , p \in \mathbb{Z}^+ \quad (64)$$

$$= \int_0^1 \frac{1}{t^{p+1} e^t} dt + \int_1^{\infty} \frac{1}{t^{p+1} e^t} dt \quad (65)$$

Consider the integral

$$I = \int_0^1 \frac{1}{t^{p+1}} dt = \lim_{a \rightarrow 0^+} \int_a^1 \frac{1}{t^{p+1}} dt \quad (66)$$

$$= \lim_{a \rightarrow 0^+} \left[\frac{t^{-(p+1)}}{-(p+1)+1} \right]_a^1 \quad (67)$$

$$= \lim_{a \rightarrow 0^+} \left[\frac{-t^{-(p+1)}}{p} \right]_a^1 \quad (68)$$

$$= \lim_{a \rightarrow 0^+} \left[\frac{-1}{p} + \frac{1}{a^{p+1} p} \right] \quad (69)$$

$$= \frac{-1}{p} + \lim_{a \rightarrow 0^+} \frac{1}{a^{p+1} p} \quad (70)$$

$$= \frac{-1}{p} + \infty \quad (71)$$

$$= \infty \quad (72)$$

Since I diverges,

$$\int_0^1 \frac{1}{t^{p+1} e^t} dt$$

also diverges by integral comparison test. And likewise, consider the integral:

$$J = \int_1^\infty \frac{1}{e^t} dt = \lim_{a \rightarrow \infty} \int_1^a e^{-t} dt \quad (73)$$

$$= \lim_{a \rightarrow \infty} \left[-e^{-t} \right]_1^a \quad (74)$$

$$= \lim_{a \rightarrow \infty} \left[\frac{-1}{e^a} + \frac{1}{e} \right] \quad (75)$$

$$= 0 + \frac{1}{e} \quad (76)$$

$$= \frac{1}{e} \quad (77)$$

Since J converges, $\int_1^\infty \frac{1}{t^{p+1} e^t} dt$ also converges by the integral comparison test Hence,

$$\int_0^1 \frac{1}{t^{p+1} e^t} dt + \int_1^\infty \frac{1}{t^{p+1} e^t} dt = \infty + \frac{1}{e} \quad (78)$$

$$= \infty \quad (79)$$

i.e. $\Gamma(-p)$ diverges for $p \in \mathbb{Z}^+$

TODO show that $\frac{1}{\Gamma(-p)} = 0 \forall p > 0$

General Proof In sections A.4 and A.4 it was shown that a recurrence relation can be related to an ODE and then that solution can be transformed to provide a solution for the recurrence relation. This was shown in two separate cases, one with unique roots and the other with repeated roots. However, in many circumstances the solutions to the characteristics equation are a combination of both unique and repeated roots. Hence, in general the solution to a linear ODE will be a superposition of solutions for each root, repeated or unique and so a goal of our research will be to put this together to find a general solution for homogenous linear recurrence relations.

Sketching out an approach for this:

- Use the Generating function to get an ODE
 - The ODE will have a solution that is a combination of the above two forms
 - The solution will translate back to a combination of both above forms
1. Power Series Combination

References

- [1] *Astropy*. URL: <https://www.astropy.org/> (visited on 10/20/2020) (cit. on p. 19).
- [2] Michael Bader. *Space-Filling Curves: An Introduction with Applications in Scientific Computing*. Texts in Computational Science and Engineering 9. Heidelberg ; New York: Springer, 2013. 278 pp. ISBN: 978-3-642-31045-4 (cit. on p. 6).
- [3] Benedetta Palazzo. *The Numbers of Nature: The Fibonacci Sequence*. June 27, 2016. URL: <http://www.eniscuola.net/en/2016/06/27/the-numbers-of-nature-the-fibonacci-sequence/> (visited on 08/28/2020) (cit. on p. 29).
- [4] Jeff Bezanson et al. “Julia: A Fresh Approach to Numerical Computing”. In: *SIAM Review* 59.1 (Jan. 2017), pp. 65–98. ISSN: 0036-1445, 1095-7200. DOI: [10.1137/141000671](https://doi.org/10.1137/141000671). URL: <https://pubs.siam.org/doi/10.1137/141000671> (visited on 08/28/2020) (cit. on p. 13).
- [5] John Bohannon. *Sunflowers Show Complex Fibonacci Sequences*. May 17, 2016. URL: <https://www.sciencemag.org/news/2016/05/sunflowers-show-complex-fibonacci-sequences> (visited on 10/22/2020) (cit. on p. 37).
- [6] William Bown. *Science: Mandelbrot Set Is as Complex as It Could Be*. URL: <https://www.newscientist.com/article/mgl3117882-900-science-mandelbrot-set-is-as-complex-as-it-could-be/> (visited on 10/22/2020) (cit. on p. 53).
- [7] Simon Brass. *CC Search*. 2006, September 5. URL: <https://search.creativecommons.org/> (visited on 08/28/2020) (cit. on p. 37).
- [8] John Briggs and F. David Peat. *Turbulent Mirror: An Illustrated Guide to Chaos Theory and the Science of Wholeness*. 1st ed. New York: Harper & Row, 1989. 222 pp. ISBN: 978-0-06-016061-6 (cit. on p. 34).
- [9] Peter Brown et al. *History and Applications - Fibonacci Numbers*. Aug. 2, 2019. URL: https://amsi.org.au/ESA_Senior_Years/SeniorTopic1/1d/1d_4history_2.html (visited on 10/22/2020) (cit. on p. 34).
- [10] Ruel V. Churchill and James Ward Brown. *Complex Variables and Applications*. Ninth Edition. Brown and Churchill Series. New York, NY: McGraw-Hill Education, 2014. 461 pp. ISBN: 978-0-07-338317-0 (cit. on p. 35).
- [11] *CTAN: Package Animate*. URL: <https://ctan.org/pkg/animate?lang=en> (visited on 10/21/2020) (cit. on p. 3).
- [12] Gerald A. Edgar. *Measure, Topology, and Fractal Geometry*. 2nd ed. Undergraduate Texts in Mathematics. New York: Springer-Verlag, 2008. 268 pp. ISBN: 978-0-387-74748-4 (cit. on pp. 3, 4, 7, 56).
- [13] Gerald A. Edgar. *Measure, Topology, and Fractal Geometry*. 2nd ed. Undergraduate Texts in Mathematics. New York: Springer-Verlag, 2008. 268 pp. ISBN: 978-0-387-74748-4 (cit. on p. 8).
- [14] K. J. Falconer. *Fractal Geometry: Mathematical Foundations and Applications*. 2nd ed. Chichester, England: Wiley, 2003. 337 pp. ISBN: 978-0-470-84861-6 978-0-470-84862-3 (cit. on pp. 4, 5, 8, 11, 43, 56).

REFERENCES

- [15] K. J. Falconer. *Fractal Geometry: Mathematical Foundations and Applications*. 2nd ed. Chichester, England: Wiley, 2003. 337 pp. ISBN: 978-0-470-84861-6 978-0-470-84862-3 (cit. on p. 11).
- [16] Peter Farrell. *Math Adventures with Python: An Illustrated Guide to Exploring Math with Code*. San Francisco: No Starch Press, 2019. 276 pp. ISBN: 978-1-59327-867-0 (cit. on p. 40).
- [17] *Fractal*. In: *Wikipedia*. Sept. 15, 2020. URL: <https://en.wikipedia.org/w/index.php?title=Fractal&oldid=978464038> (visited on 10/19/2020) (cit. on p. 4).
- [18] Robert Gilmore and Marc Lefranc. *The Topology of Chaos: Alice in Stretch and Squeezeland*. New York: Wiley-Interscience, 2002. 495 pp. ISBN: 978-0-471-40816-1 (cit. on p. 5).
- [19] Frank R. Giordano, William P. Fox, and Steven B. Horton. *A First Course in Mathematical Modeling*. 5th ed., International ed. Australia ; Boston, MA: Brooks/Cole, Cengage Learning, 2014. 676 pp. ISBN: 978-1-285-05090-4 978-1-285-07749-9 (cit. on p. 34).
- [20] Ralph Gomory. “Benoît Mandelbrot (1924–2010)”. In: *Nature* 468.7322 (7322 Nov. 2010), pp. 378–378. ISSN: 1476-4687. DOI: [10.1038/468378a](https://doi.org/10.1038/468378a). URL: <https://www.nature.com/articles/468378a> (visited on 10/19/2020) (cit. on pp. 3, 4).
- [21] Jean-François Gouyet. *Physics and Fractal Structures*. Paris : New York: Masson ; Springer, 1996. 234 pp. ISBN: 978-0-387-94153-0 978-3-540-94153-8 978-2-225-85130-8 (cit. on pp. 4, 5, 25, 57).
- [22] Ronald L. Graham, Donald Ervin Knuth, and Oren Patashnik. *Concrete Mathematics: A Foundation for Computer Science*. 2nd ed. Reading, Mass: Addison-Wesley, 1994. 657 pp. ISBN: 978-0-201-55802-9 (cit. on p. 8).
- [23] jan wassenaar. *Cantor Dust*. Jan. 7, 2005. URL: <http://www.2dcurves.com/fractal/fractald.html> (visited on 10/20/2020) (cit. on p. 13).
- [24] Junwei Jiang and Roy E. Plotnick. “Fractal Analysis of the Complexity of United States Coastlines”. In: *Mathematical Geology* 30.5 (July 1, 1998), pp. 535–546. ISSN: 1573-8868. DOI: [10.1023/A:1021790111404](https://doi.org/10.1023/A:1021790111404). URL: <https://doi.org/10.1023/A:1021790111404> (visited on 10/19/2020) (cit. on p. 4).
- [25] *Julia Set*. In: *Wikipedia*. July 12, 2020. URL: https://en.wikipedia.org/w/index.php?title=Julia_set&oldid=967264809 (visited on 08/25/2020) (cit. on p. 43).
- [26] *JuliaAstro · JuliaAstro*. URL: <https://juliaastro.github.io/dev/index.html> (visited on 10/20/2020) (cit. on p. 19).
- [27] *JuliaGraphics/Luxor.jl*. JuliaGraphics, Oct. 19, 2020. URL: <https://github.com/JuliaGraphics/Luxor.jl> (visited on 10/20/2020) (cit. on p. 19).
- [28] *JuliaImages/Images.jl*. JuliaImages, Oct. 13, 2020. URL: <https://github.com/JuliaImages/Images.jl> (visited on 10/20/2020) (cit. on p. 19).

REFERENCES

- [29] Robert Lamb. *How Are Fibonacci Numbers Expressed in Nature?* June 24, 2008. URL: <https://science.howstuffworks.com/math-concepts/fibonacci-nature.htm> (visited on 08/28/2020) (cit. on p. 29).
- [30] Ron Larson and Bruce H. Edwards. *Elementary Linear Algebra*. 2nd ed. Lexington, Mass: D.C. Heath, 1991. 592 pp. ISBN: 978-0-669-24592-9 (cit. on p. 5).
- [31] Eric Lehman, Tom Leighton, and Albert Meyer. *Readings / Mathematics for Computer Science / Electrical Engineering and Computer Science / MIT OpenCourseWare*. Sept. 8, 2010. URL: <https://ocw.mit.edu/courses/electrical-engineering-and-computer-science/6-042j-mathematics-for-computer-science-fall-2010/readings/> (visited on 08/10/2020) (cit. on p. 60).
- [32] Oscar Levin. *Solving Recurrence Relations*. Jan. 29, 2018. URL: http://discrete.openmathbooks.org/dmoi2/sec_recurrence.html (visited on 08/11/2020) (cit. on p. 62).
- [33] Zhong Li, Wolfgang A. Halang, and G. Chen, eds. *Integration of Fuzzy Logic and Chaos Theory*. Studies in Fuzziness and Soft Computing v. 187. Berlin ; New York: Springer, 2006. 625 pp. ISBN: 978-3-540-26899-4 (cit. on p. 7).
- [34] *List of Fractals by Hausdorff Dimension*. In: *Wikipedia*. Sept. 8, 2020. URL: https://en.wikipedia.org/w/index.php?title=List_of_fractals_by_Hausdorff_dimension&oldid=977401154 (visited on 09/24/2020) (cit. on p. 11).
- [35] ImageMagick Studio LLC. *ImageMagick*. URL: <https://imagemagick.org/> (visited on 10/20/2020) (cit. on p. 19).
- [36] Benoit Mandelbrot. “How Long Is the Coast of Britain? Statistical Self-Similarity and Fractional Dimension”. In: *Science* 156.3775 (May 5, 1967), pp. 636–638. ISSN: 0036-8075, 1095-9203. DOI: [10.1126/science.156.3775.636](https://doi.org/10.1126/science.156.3775.636). PMID: [17837158](https://pubmed.ncbi.nlm.nih.gov/17837158/). URL: <https://science.sciencemag.org/content/156/3775/636> (visited on 10/19/2020) (cit. on p. 4).
- [37] Benoit B. Mandelbrot. *The Fractal Geometry of Nature*. San Francisco: W.H. Freeman, 1982. 460 pp. ISBN: 978-0-7167-1186-5 (cit. on pp. 3–5, 14).
- [38] Benoit B. Mandelbrot and Richard L. Hudson. *The (Mis)Behaviour of Markets: A Fractal View of Risk, Ruin, and Reward*. Pbk. ed. London: Profile, 2008. 326 pp. ISBN: 978-1-84668-262-9 (cit. on p. 4).
- [39] Mark Pollicott. *Fractals and Dimension Theory*. 2005-May. URL: https://warwick.ac.uk/fac/sci/maths/people/staff/mark_pollicott/p3 (cit. on p. 11).
- [40] A Mathai and T Davis. “Constructing the Sunflower Head”. In: *Mathematical Biosciences* 20.1-2 (June 1, 1974), pp. 117–133. ISSN: 0025-5564. DOI: [10.1016/0025-5564\(74\)90072-8](https://doi.org/10.1016/0025-5564(74)90072-8). URL: <https://www.sciencedirect.com/science/article/pii/0025556474900728> (visited on 10/22/2020) (cit. on p. 37).
- [41] Curtis T. McMullen. “Hausdorff Dimension and Conformal Dynamics, III: Computation of Dimension”. In: *American Journal of Mathematics* 120.4 (1998), pp. 691–721. ISSN: 0002-9327. JSTOR: [25098619](https://doi.org/10.2307/2321375) (cit. on p. 50).
- [42] Nikoletta Minarova. “The Fibonacci Sequence: Nature’s Little Secret”. In: *CRIS - Bulletin of the Centre for Research and Interdisciplinary Study* 2014.1 (2014), pp. 7–17. ISSN: 1805-5117 (cit. on p. 29).

REFERENCES

- [43] Derick Muller, director. *This Equation Will Change How You See the World (the Logistic Map)*. Jan. 29, 2020. URL: <https://www.youtube.com/watch?v=ovJcsL7vyrk&vl=en> (visited on 10/22/2020) (cit. on p. 34).
- [44] *Nature, The Golden Ratio and Fibonacci Numbers*. 2018. URL: <https://www.mathsisfun.com/numbers/nature-golden-ratio-fibonacci.html> (visited on 08/28/2020) (cit. on pp. 29, 37, 38).
- [45] Olympia Nicodemi, Melissa A. Sutherland, and Gary W. Towsley. *An Introduction to Abstract Algebra with Notes to the Future Teacher*. Upper Saddle River, NJ: Pearson Prentice Hall, 2007. 436 pp. ISBN: 978-0-13-101963-8 (cit. on p. 62).
- [46] *Pdftex - Is There Any Way to Include an Animated GIF Directly?* URL: <https://tex.stackexchange.com/questions/5396/is-there-any-way-to-include-an-animated-gif-directly> (visited on 10/21/2020) (cit. on p. 3).
- [47] Heinz-Otto Peitgen, H. Jürgens, and Dietmar Saupe. *Chaos and Fractals: New Frontiers of Science*. 2nd ed. New York: Springer, 2004. 864 pp. ISBN: 978-0-387-20229-7 (cit. on pp. 5, 14, 22, 40, 51, 53, 57).
- [48] *Pillow—Pillow (PIL Fork) 8.0.0 Documentation*. URL: <https://pillow.readthedocs.io/en/stable/> (visited on 10/20/2020) (cit. on p. 19).
- [49] Guru Prasad. *How Fibonacci Number Series Originated in Ancient India*. Sept. 22, 2018. URL: <http://guruprasad.net/posts/fibonacci-number-series-originated-ancient-india/> (visited on 10/22/2020) (cit. on p. 34).
- [50] R Core Team. *R: A Language and Environment for Statistical Computing*. manual. R Foundation for Statistical Computing. Vienna, Austria, 2020. URL: <https://www.R-project.org/> (cit. on p. 13).
- [51] J Ridley. “Packing Efficiency in Sunflower Heads”. In: *Mathematical Biosciences* 58.1 (Feb. 1, 1982), pp. 129–139. ISSN: 0025-5564. DOI: [10.1016/0025-5564\(82\)90056-6](https://doi.org/10.1016/0025-5564(82)90056-6). URL: <http://www.sciencedirect.com/science/article/pii/0025556482900566> (visited on 10/22/2020) (cit. on p. 37).
- [52] Ron Knott. *The Fibonacci Numbers and Golden Section in Nature - 1*. Sept. 25, 2016. URL: <http://www.maths.surrey.ac.uk/hosted-sites/R.Knott/Fibonacci/fibnat.html> (visited on 08/28/2020) (cit. on pp. 29, 34).
- [53] Grant Sanderson, director. *Fractals Are Typically Not Self-Similar*. Jan. 27, 2017. URL: https://www.youtube.com/watch?v=gB9n2gHsHN4&lc=Ugj8mIhm_S17y3gCoAEC (visited on 10/19/2020) (cit. on pp. 3, 5, 6, 8, 25).
- [54] Shelly Allen. *Fibonacci in Nature*. URL: <https://fibonacci.com/nature-golden-ratio/> (visited on 08/28/2020) (cit. on p. 29).
- [55] Steven H. Strogatz. *Nonlinear Dynamics and Chaos: With Applications to Physics, Biology, Chemistry, and Engineering*. Second edition. Boulder, CO: Westview Press, a member of the Perseus Books Group, 2015. 513 pp. ISBN: 978-0-8133-4910-7 (cit. on p. 6).
- [56] Sergei Tabachnikov. “Dragon Curves Revisited”. In: *The Mathematical Intelligencer* 36.1 (Feb. 2014), pp. 13–17. ISSN: 0343-6993, 1866-7414. DOI: [10.1007/s00283-013-9428-y](https://doi.org/10.1007/s00283-013-9428-y). URL: <http://link.springer.com/10.1007/s00283-013-9428-y> (visited on 10/20/2020) (cit. on p. 22).

REFERENCES

- [57] Tamás Tél, Márton Gruiz, and Katalin Kulacsy. *Chaotic dynamics: an introduction based on classical mechanics*. Cambridge: Cambridge University Press, 2006. ISBN: 9780511335044 9780511334467 9780511333125 9780511803277 9780511333804 9781281040114 9786611040116 9780511567216. URL: <https://doi.org/10.1017/CBO9780511803277> (visited on 08/28/2020) (cit. on pp. 3, 57).
- [58] Jeffrey Ventrella. *Space-Filling Curves Are Not Squares*. Nov. 16, 2014. URL: <https://spacefillingcurves.wordpress.com/2014/11/16/space-filling-curves-are-not-squares/> (visited on 10/20/2020) (cit. on p. 22).
- [59] Tamás Vicsek. *Fractal Growth Phenomena*. 2nd ed. Singapore ; New Jersey: World Scientific, 1992. 488 pp. ISBN: 978-981-02-0668-0 978-981-02-0669-7 (cit. on pp. 3, 13, 25, 57).
- [60] Helmut Vogel. “A Better Way to Construct the Sunflower Head”. In: *Mathematical Biosciences* 44.3-4 (June 1, 1979), pp. 179–189. ISSN: 0025-5564. DOI: [10.1016/0025-5564\(79\)90080-4](https://doi.org/10.1016/0025-5564(79)90080-4). URL: <http://www.sciencedirect.com/science/article/pii/0025556479900804> (visited on 10/22/2020) (cit. on p. 37).
- [61] *Welcome to Python.Org*. URL: <https://www.python.org/> (visited on 10/20/2020) (cit. on p. 13).
- [62] Xiaojing Zhong, Peng Yu, and Shenliang Chen. “Fractal Properties of Shoreline Changes on a Storm-Exposed Island”. In: *Scientific Reports* 7.1 (1 Aug. 15, 2017), p. 8274. ISSN: 2045-2322. DOI: [10.1038/s41598-017-08924-9](https://doi.org/10.1038/s41598-017-08924-9). URL: <https://www.nature.com/articles/s41598-017-08924-9> (visited on 10/19/2020) (cit. on p. 4).
- [63] Xiao-hua Zhu and Jian Wang. “On Fractal Mechanism of Coastline”. In: *Chinese Geographical Science* 12.2 (June 1, 2002), pp. 142–145. ISSN: 1993-064X. DOI: [10.1007/s11769-002-0022-z](https://doi.org/10.1007/s11769-002-0022-z). URL: <https://doi.org/10.1007/s11769-002-0022-z> (visited on 10/19/2020) (cit. on p. 4).
- [64] Dennis G Zill and Michael R Cullen. *Differential Equations*. 7th ed. Brooks/Cole, 2009 (cit. on pp. 61, 62).
- [65] Dennis G. Zill and Michael R. Cullen. “8.4 Matrix Exponential”. In: *Differential Equations with Boundary-Value Problems*. 7th ed. Belmont, CA: Brooks/Cole, Cengage Learning, 2009. ISBN: 978-0-495-10836-8 (cit. on pp. 62, 64).
- [66] Dennis G. Zill and Michael R. Cullen. *Differential Equations with Boundary-Value Problems*. 7th ed. Belmont, CA: Brooks/Cole, Cengage Learning, 2009. 526 pp. ISBN: 978-0-495-10836-8 (cit. on p. 35).